A SYSTEMATIC INVESTIGATION OF SHEAR CONNECTIONS BETWEEN FULL-DEPTH PRECAST PANELS AND PRECAST PRESTRESSED BRIDGE GIRDERS

A Thesis

by

ROBERT WAYNE BREY JR.

Submitted to the Office of Graduate Studies of
Texas A&M University
in partial fulfillment of the requirements for the degree of

MASTER OF SCIENCE

May 2010

Major Subject: Civil Engineering

A SYSTEMATIC INVESTIGATION OF SHEAR CONNECTIONS BETWEEN FULL-DEPTH PRECAST PANELS AND PRECAST PRESTRESSED BRIDGE GIRDERS

A Thesis

by

ROBERT WAYNE BREY JR.

Submitted to the Office of Graduate Studies of
Texas A&M University
in partial fulfillment of the requirements for the degree of

MASTER OF SCIENCE

Approved by:

Chair of Committee,	John Mander
Committee Members,	Monique Hite Head
	Hanifah Muliana
Head of Department,	John Niedzwecki

May 2010

Major Subject: Civil Engineering

ABSTRACT

A Systematic Investigation of Shear Connections Between Full-Depth Precast Panels and Precast Prestressed Bridge Girders. (May 2010)

Robert Wayne Brey Jr., B.S., Texas A&M University

Chair of Advisory Committee: Dr. John Mander

Full-depth precast panels are used in concrete bridges to provide several benefits such as faster construction, lower cost and reduced constructional hazard. However, one construction drawback is that connectors are required to transmit horizontal shear across the interface between the girder and deck. Shear connector performance is characterized by a series of experiments performed on part of a bridge system that mimics a full-depth precast deck on concrete girder with a pocket-connector-haunch system. Following initial breakaway of the adhesive bond within the haunch region, the specimens slide with frictional resistance provided by the clamping force of the anchor bolt. This leads to bolt yield with an observed sliding friction coefficient of 0.8 ($\pm$20%) with lower values occurring at higher displacements. It is concluded that for a viable connector system to be developed a key feature is to have sufficient stirrups in the neighborhood of the anchor bolt to form a non-contact splice and to ensure the high pull-out force can be sustained without leading to premature beam failure.

The successful implementation of a full-depth precast deck-panel system requires the use of a viable design methodology that properly accounts for *system* behavior. The

design of a deck-haunch-girder system uses a truss modeling approach to design for the shear forces created by service loading. The truss model approach is considered more suitable for a concrete member due to the premise that the member will be substantially cracked at an ultimate limit state and that traditional beam theory does not account for the decreased ability of shear stresses to transfer across open cracks. Experimental results from Chapter II, such as the friction coefficient μ, are used along with a previously developed crack angle model to layout the geometry of the truss within a deck-panel span. Design solutions are presented utilizing the Rock Creek Bridge in Parker County, Texas as an example structure.

ACKNOWLEDGEMENTS

I would like to thank Dr. John Mander, my advisor, and my committee members, Dr. Monique Head from the Civil Engineering Department, and Dr. Anastasia Muliana from the Mechanical Engineering Department for sharing their experience, support and guidance through this journey.

I would like to thank Thomas Mander and Reece Scott for their help with construction and pours throughout the project. I also thank the High Bay Structural and Materials Testing Laboratory, Dr. Peter Keating, and Matt Potter for their flexibility and assistance with the lab operations.

I would also like to thank Troy Stephan from the Nuclear Engineering Shop along with his students Alex and Travis for their time, help, and sharing their machine work knowledge with me.

Finally, for their prayers and support, I would like to thank my family and friends, especially my wife, Jennifer.

NOMENCLATURE

AASHTO	American Association of State Highway Transportation Officials
ACI	American Concrete Institute
As_{con}	Total cross-sectional area of shear connectors in a pocket
A_{sh}	Cross-sectional area of a single transverse hoop
BMSPx	String pot – beam vertical displacment
CIP	Cast-in-place
CR	Coil rod
LFLC	Load cell – lateral force
L_{panel}	Length of a panel
LVDT	Linear variable differential transducer
LVR	LVDT – deck horizontal displacement, right side
LVL	LVDT – deck horizontal displacement, left side
N_{group}	Number of hoops required to anchor shear connectors in a pocket
N_{Pocket}	Number of pocket per panel
SGC	Strain gauge – compression side
SGT	Strain gauge – tension side
SIP	Stay-in-place
SP	String potentiometer
SPTD	String pot – total displacement
SPVRx	String pot – vertical displacement, right side

SPVLx	String pot – vertical displacement, left side
TDLC	Load cell – tied down force
TR	Threaded rod
TRH	Threaded rod with side-by-side configuration
TXDOT	Texas Department of Transportation
f'_c	Concrete compressive strength
fy_{sh}	Transverse reinforcement yield strength
fy_{con}	Shear connector yield strength
jd_{girder}	Internal lever arm within the girder
jd_o	Overall internal lever arm
w/p	Water to powder ratio

TABLE OF CONTENTS

CHAPTER Page

LIST OF FIGURES

FIGURE Page

LIST OF TABLES

CHAPTER I

INTRODUCTION

1.1 Background and Motivation

Reduced construction time is a desire of each party involved in an engineering project. Bridge construction is no exception to this as it can affect numerous people with traffic delays and road closures. Accelerated forms of bridge construction can provide a reduction in construction time.

Many current highway bridges are constructed using concrete decks placed on steel or precast concrete girders. These decks usually consist of precast concrete panels that span the interior girders of the bridge which act as the formwork for the cast-in-place (CIP) portion of the deck. The overhangs of the bridge deck must be formed with wood and the full-depth of the deck at the overhang is obtained with one pour. The time to place the formwork and reinforcing steel on the overhang portion of the bridge costs valuable time in the bridge construction process. This can be eliminated through the use of a precast full-depth deck panel that can simply be placed on the exterior girders and provide the full-depth deck overhang. The remaining element in this type of construction is the connection between the full-depth deck panel and precast concrete girder.

Shear connectors can be used to form a load path which transmits horizontal

---

This thesis follows the style of *Journal of Structural Engineering*.

shear between the girder and deck which provides composite action and gives an efficient section. The main goals of this thesis are:

1. Acquire the horizontal load-displacement performance for various shear connectors specimens.
2. Monitor the effects of the shear connection on a relatively narrow web found in common precast bridge girders.
3. Compare the performance of a coil rod connector to the performance of the threaded rod connectors.
4. Present a design method for a full-depth deck-girder system.

1.2 Literature Review

A large amount of research has been performed on the topic of shear connections in full-depth precast bridge decks. Many different connection methods and test setups have been used in past work.

Issa et al. (2006), conducted experiments on the behavior of shear connectors used with full-depth decks. Their work used modified AASHTO girder segments, shown in Fig. 1, into which the connectors were post installed. The use of an AASHTO type girder is useful as it closely replicates actual bridge girder geometry. The authors tested 1-in. bolts that were post installed into the girder utilizing several different layout configurations. The authors concluded that AASHTO LRFD Section 5.8.4.1 Equation 5.8.4.1-1 would allow for conservative design of a system similar to the one tested.

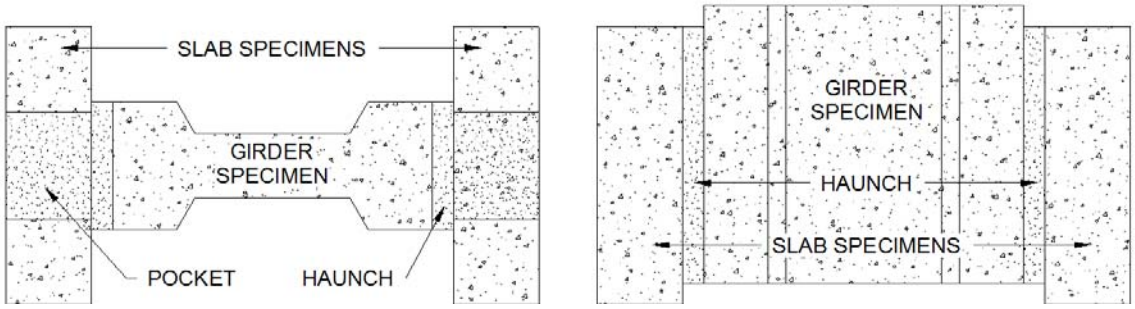

Fig. 1 – AASHTO-type stub girder test setup.

Research on behalf of the Virginia Transportation Research Council (VTRC) by Menkulasi and Roberts-Wollmann (2005), conducted 36 push-off tests to study the performance of horizontal shear connections for use with full-depth precast panels. Their experiments consisted of two L-shaped concrete elements placed on top of each other and connected with the shear connector under investigation. The double-L shaped test setup is shown in Fig. 2. The experiments examined type and size of connector, type of grout, and haunch height in order to evaluate their contribution to the connection performance. They performed tests on stirrups, hooked bars and coil inserts. It was concluded that AASHTO LRFD also provided the best estimate for design strength.

Scholz et al. (2007) investigated shear performance via 29 push-off tests and considered connector type, connector size and number, grout type, surface treatment and pocket type. This research proposed that the AASHTO LRFD provision for horizontal shear resistance be modified. The AASHTO LRFD manual permits horizontal shear capacity be calculated as a combination of cohesion and shear friction. The authors proposed that a new equation be created that separated the two mechanisms due to the fact that cohesion contributes before the haunch cracks and the shear connectors will not take over until after the haunch has cracked, removing the initial bond (cohesion). Their proposed equation was:

$$v_n = max\left|cA_{cv}, \mu\left(A_s f_y + P_n\right)\right| \quad (1)$$

where c = the cohesion (0.5 MPa, 75 psi), A_{cv} = the interface area, μ = a coefficient of friction (μ = 0.9 for grout on concrete interface, μ = 0.6 for grout on steel interface), A_s =

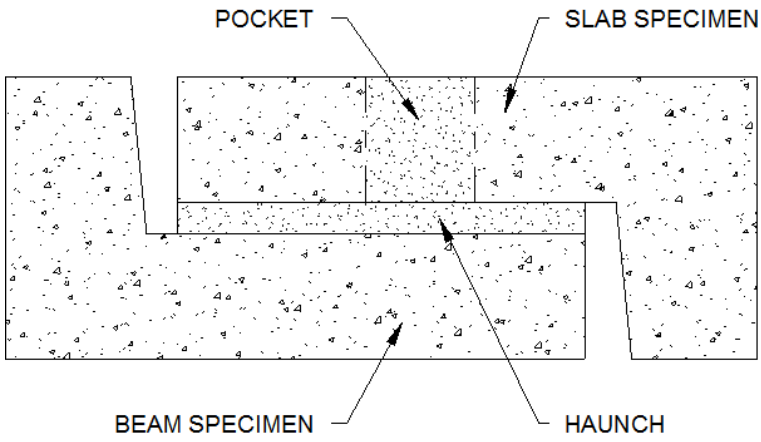

Fig. 2 – Common double-L shaped test setup.

the area of shear connector(s) crossing the interface, f_y = the connector yield stress, and P_n = the additional normal force.

The above described previous work that used the common double-L setup, in an attempt to provide pure shear with no moment, did not strictly represent a realistic loading scenario. Typical bridge girders have deck-to-girder shear in the presence of a moment gradient, which produces shear. This is discussed in more depth in the subsection 2.3 where tests described herein were conducted to represent a more realistic loading scenario to evaluate the horizontal shear on shear connector performance.

Henley (2009) performed push-off tests on 24 specimens with varied connectors, grout type, haunch height and installation method. 16 connections were precast into the girder specimen while 8 connections were installed after curing of the girder concrete. In order to ameliorate the above mentioned concern with double-L specimens, Henley's (2009) tests used a setup that more closely resembled a bridge girder-deck system. Fig. 3 shows the experimental setup used in Henley (2009). Deck segments were placed on a concrete beam and pushed-off to test the shear connections. Tests were conducted on mild reinforcing "R" bars, pre and post installed bolts, threaded rods, nelson studs, and a proprietary bolt. The post installed connections were made by drilling into the girder specimen and using various grout mixtures to anchor the connector.

Of the pre-installed connectors, some protruded out of the girder, while others utilized a coupler which allowed the top of the girder to remain flush until deck placement. The experiments revealed the need for sufficient girder shear reinforcement in the vicinity of the connectors to prevent a pull-out causing a brittle beam failure. It is not possible to observe such a failure in the double-L specimens of Scholz et al. (2007) and Menkulasi and Roberts-Wollemann (2005). Henley's (2009) experiments attempted to provide a setup that more closely represented a bridge girder, but in doing so an important detailing issue was discovered. Brittle failures seen in those experiments revealed that without proper transverse reinforcement, pull-out forces from the shear connectors cannot be adequately resisted.

1.3 Organization of Thesis

This thesis consists of chapters of similar information. In succession of this introductory chapter, Chapter II provides experimental study. Chapter III follows with the design process of shear connectors. Chapter IV consists of the conclusions and recommendations as a result of the work presented in this thesis.

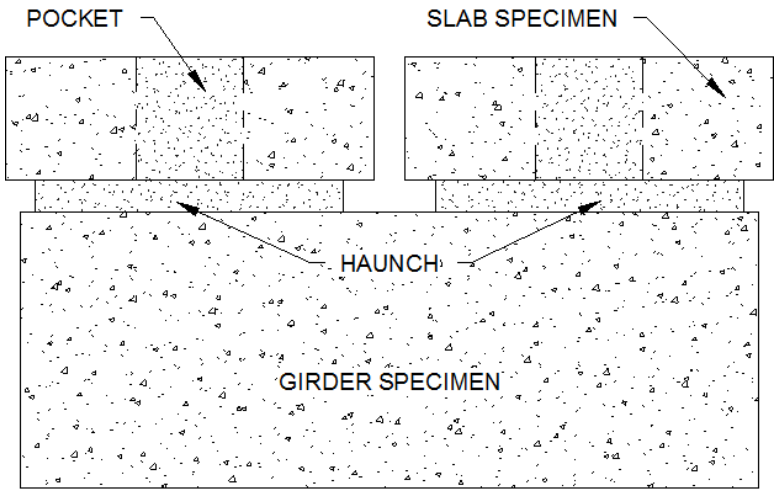

Fig. 3 – Henley (2009) test setup.

1.4 What Then Is Particularly New In This Thesis

The experimental research of this thesis offers a unique method to a common research topic. The experimental setup used in this research is of particular individuality which gives a more precise representation of a deck-haunch-girder system. This research conducted unique experiments using an I-shaped girder with realistic girder reinforcement in order to determine any negative effects from the relatively narrow web. The coil rod shear connector specimens are unique to this research as well.

This thesis provides a design method for shear connectors in a full-depth concrete deck system using a truss modeling approach.

CHAPTER II

EXPERIMENTAL INVESTIGATION

2.1 Chapter Summary

Full-depth precast panels used in concrete bridges provide several benefits such as faster construction, lower cost and reduced constructional hazard. However, one construction drawback is that connectors are required to transmit horizontal shear across the interface between the girder and deck. Shear connector performance is characterized by a series of experiments performed on part of a bridge system that mimics a full-depth precast deck on concrete girder with a pocket-connector-haunch system. Horizontal shear-displacement push-off test performance is examined. Following initial breakaway of the adhesive bond within the haunch region, the specimens slide with frictional resistance provided by the clamping force of the anchor bolt. This leads to bolt yield with an observed sliding friction coefficient of 0.8 ($\pm$20%) with lower values occurring at higher displacements. It is concluded that for a viable connector system to be developed a key feature is to have sufficient stirrups in the neighborhood of the anchor bolt to form a non-contact splice and to ensure the high pull-out force can be sustained without leading to premature beam failure.

2.2 Background Information

Construction of typical cast-in-place (CIP) bridge decks require a considerable amount of time to complete. A forming system must be installed prior to placing a mat

of reinforcing steel. The final portion of the deck is then poured and allowed to cure. One common construction technique for bridge decks takes advantage of precast concrete elements by using them for formwork. Precast elements used in this manner are usually only the lower half of the required depth for the slab. The upper half remains CIP, requiring the upper mat of reinforcing steel to be placed in the field before the final concrete is poured. A full-depth precast bridge deck removes the need to place steel and pour deck concrete on the jobsite. These processes can be done offsite with sufficient lead time to allow the deck to be ready, thereby removing the site down-time for the curing the concrete.

Stay-in-place (SIP) formwork has historically only been used for that portion of the deck between the girders; overhangs remain CIP. A solution that provides even faster construction is a fully precast deck, including the overhang. A prototype overhang system was investigated by Mander et al. (2010) and Trejo et al. (2008). Experiments on full-scale overhang deck-panels revealed that a full-depth overhang panel provides adequate performance under AASHTO code requirements.

The downside to full-depth precast bridge deck construction is that if necessary horizontal shear resistance measures are not taken, adequate composite action between the deck and girder may not be achieved. These necessary measures require a means of connecting the precast deck to the precast girder and thereby allowing composite action to occur between the deck and girder, which provides an efficient section. A way to accomplish this connection is with the use of isolated shear connectors housed in "pockets" formed within the precast deck panels. These connectors must have sufficient

shear strength in order to form a load path to the deck but also remain stable throughout loading to prevent damage to the girder. The connector portion housed in the deck is connected to a companion piece that is precast into the girder. The two are connected together via a coupler, which is also precast into the girder. The pocket is then filled with grout to complete the girder-deck joint.

In this paper an experimental study is conducted that investigates the lateral strength of the deck-to-girder system that includes all the full scale details of reinforcement and interface grout. Previous experimental work, reviewed below, has generally used a double-L-shaped type of shear specimen. In this research, it is contended that such an experimental approach is not sufficient in discovering the interaction between the deck, the grout, and the girder along with the shear connectors—particularly given the fact that this must be in the presence of a moment gradient. Therefore, a more realistic representation of prototype conditions is developed and used for the experimental system. The experimental system also examines the effect of girder type—that is, whether a broad or narrow-web exists in the girder and its influence on performance. This paper accordingly presents and discusses the experimental results of 8 full-size horizontal shear displacement push-off tests. Design recommendations are also given.

2.3 Experimental Study

The theoretical basis for the experimental investigation presented herein is shown diagrammatically in Figs. 4 and 5. Fig. 4 presents a line of reasoning that would lead

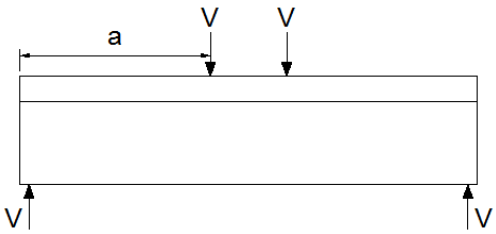

(a) Un-cracked structural concrete

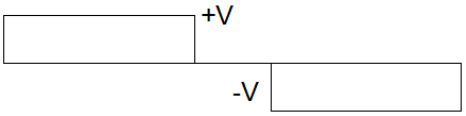

(b) Shear force diagram

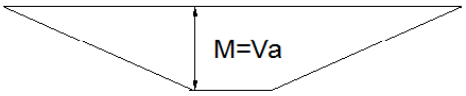

(c) Bending moment diagram

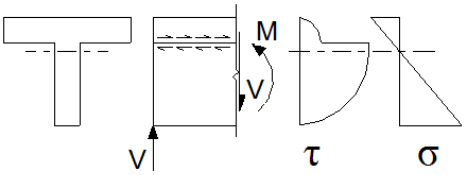

(d) Shear and direct stress analysis

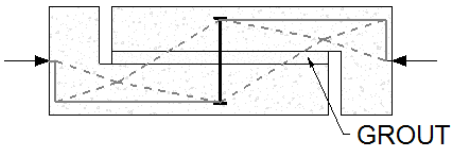

(e) Suitable method for direct shear test

Fig. 4 – Classic beam theory representation of uncracked deck-girder system.

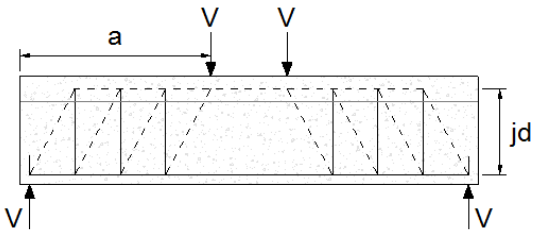

(a) Cracked structural concrete

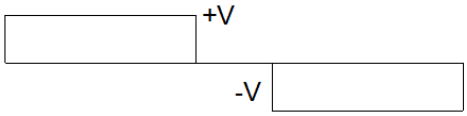

(b) Vertical force component of the truss elements

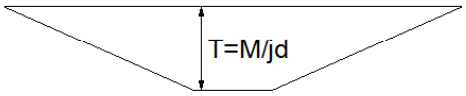

(c) Bottom tension chord force diagram

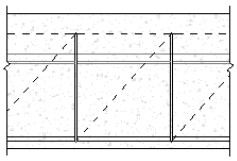

(d) Cast-in-place with stirrups

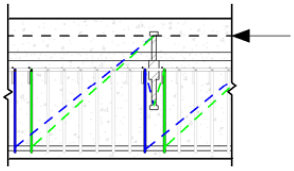

(e) Precast deck with shear connectors

Fig. 5 – Truss model representation of cracked deck-girder system.

one to believe that the double-L specimen may be a satisfactory and simple means by which testing can be conducted. From the loaded uncracked beam (Fig. 4a) shear forces and moments result (Fig. 4b and 4c), from which shear and direct stress can be calculated (Fig. 4d). The common double L-shaped test setup shown in Fig. 4(e) has been used to test direct shear, as it attempts to remove moment from the experiment. This method is an acceptable approximate representation of an uncracked concrete member. This approach however, although useful for an uncracked section, is not appropriate at an ultimate limit state at which point the section is expected to have cracked substantially. A design at the ultimate limit state should make use of a truss model.

Menkulasi and Roberts-Wollemann (2005) did indeed use a truss model in their paper to indicate the force flow of that setup and this is shown in Fig. 4(e). An anti-symmetric truss model results with compression struts forming at both sides of the anchorage. It is contended that this is an unrealistic representation of a bridge deck in light of what follows.

Fig. 5 outlines, on the other hand, an alternative line of thinking predicated on the fact that in the ultimate limit state it is inevitable that a composite structural concrete beam member will be cracked. Thus, instead of beam theory, a truss model is considered more appropriate, but this must be modeled for the whole system. The shear is resisted by a series of struts and ties formed in the concrete and transverse reinforcing steel respectively. The shear force diagram (from Fig. 4b) now becomes the vertical force component diagram for the web members of the truss (Fig. 5b), while the bending

moment diagram (from Fig. 4c) now represents the tension force diagram for the bottom chord of the truss (Fig. 5c).

Figs. 5(d) and 5(e) show a conventional cast-in-place system with stirrups and a precast deck system with shear connectors, respectively. In contrast to Fig. 4(e) which shows an anti-symmetric truss model resisting the shear in the vicinity of the anchorage, Fig. 5(e) shows an asymmetric truss with a set of compound struts that can act on only one-side of the anchorage; the moment in effect causes the other side of the slab to uplift, which more closely resembles the mechanics in a physical bridge system.

The conceptual theory behind Fig. 5(e) is applied in Fig. 6(a) to a prototype structure that shows the proposed flow of internal forces within two pockets engaged within a panel at the end of a span. It is evident from this figure that the shear connector must act, in part, as a non-contact splice. This conceptual theory is now used to provide the experimental basis for constructing the test specimens used in this research. From Fig. 6(a), the layout of the test specimens is shown in Fig. 6(b) as used in the laboratory experimental investigation. This gives internal forces for laboratory tests 1 and 3, and Fig. 6(c) presents internal forces for laboratory tests 2 and 4. Naturally laboratory space and equipment, constructability, and rate of testing also played a role in the design of the experiments.

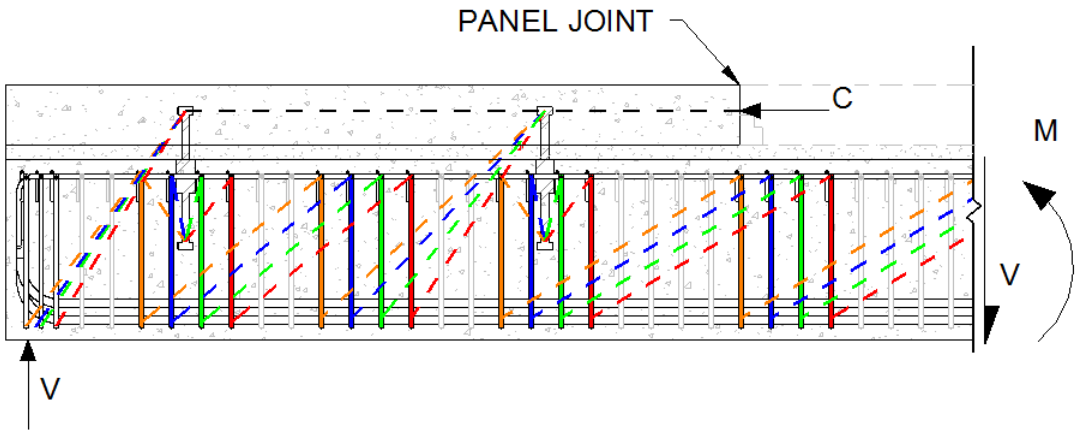

(a) Force flow for end panel with two pockets for a prototype deck-girder system

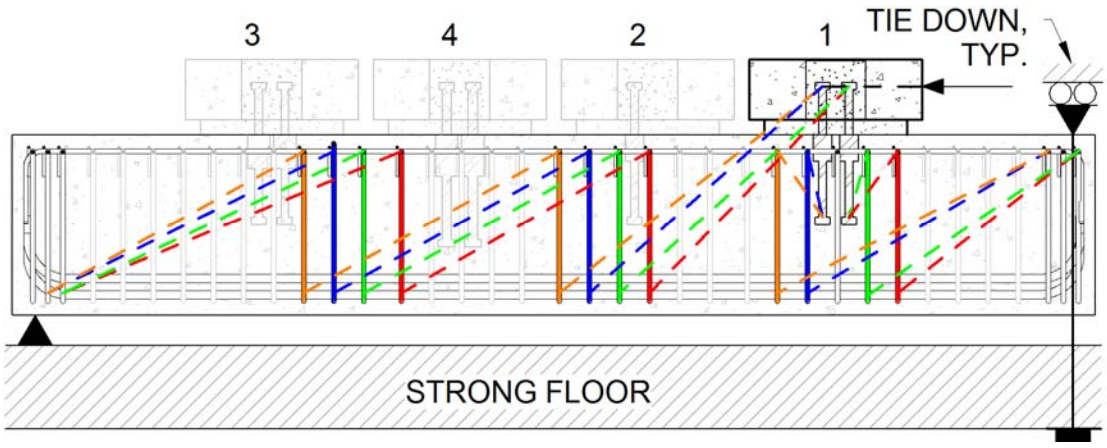

(b) Force flow for laboratory tests 1 & 3

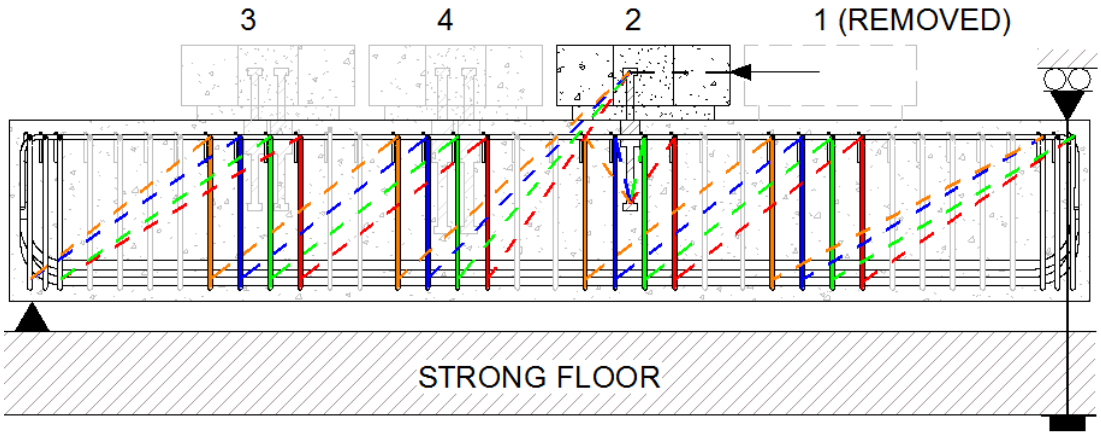

(c) Force flow for laboratory tests 2 & 4

Fig. 6 – Schematics of internal force flows in a full-depth precast bridge deck with shear connector system.

2.4 Experiment Fabrication

Fig. 7 presents the details of the two test beams and their anchor-bolt attached concrete push-off specimens along with the instrumentation layout.

2.4.1 Beam specimen details

Two beam geometries were used in the experiments of this research, a rectangular beam and an I-shaped girder. In order to provide common ground for comparison, the rectangular beam geometry was chosen similar to geometry used in the work of Henley (2009). The I-shaped section was formed by taking portions of prestressed I-shape girders used in practice and combining them into an I-section. The adopted I-section shape was based on a combination of adverse geometric conditions used in typical existing girders. This included a narrow flange and a narrow web to ensure that the shear connectors could be placed in the cage and that any potential negative performance effects could be observed.

The beam specimens used transverse shear reinforcement details similar to details given by the Texas Department of Transportation (TXDOT, 2009). To ensure proper functioning of the non-contact splice, the transverse hoops bars were bent from #5 rebars instead of the usual #4 R-bars specified by TXDOT. The beams also had top longitudinal reinforcement similar to what is specified by TXDOT in order to maintain a realistic condition for the placement of connectors among reinforcement that would be typical in prestressed girders.

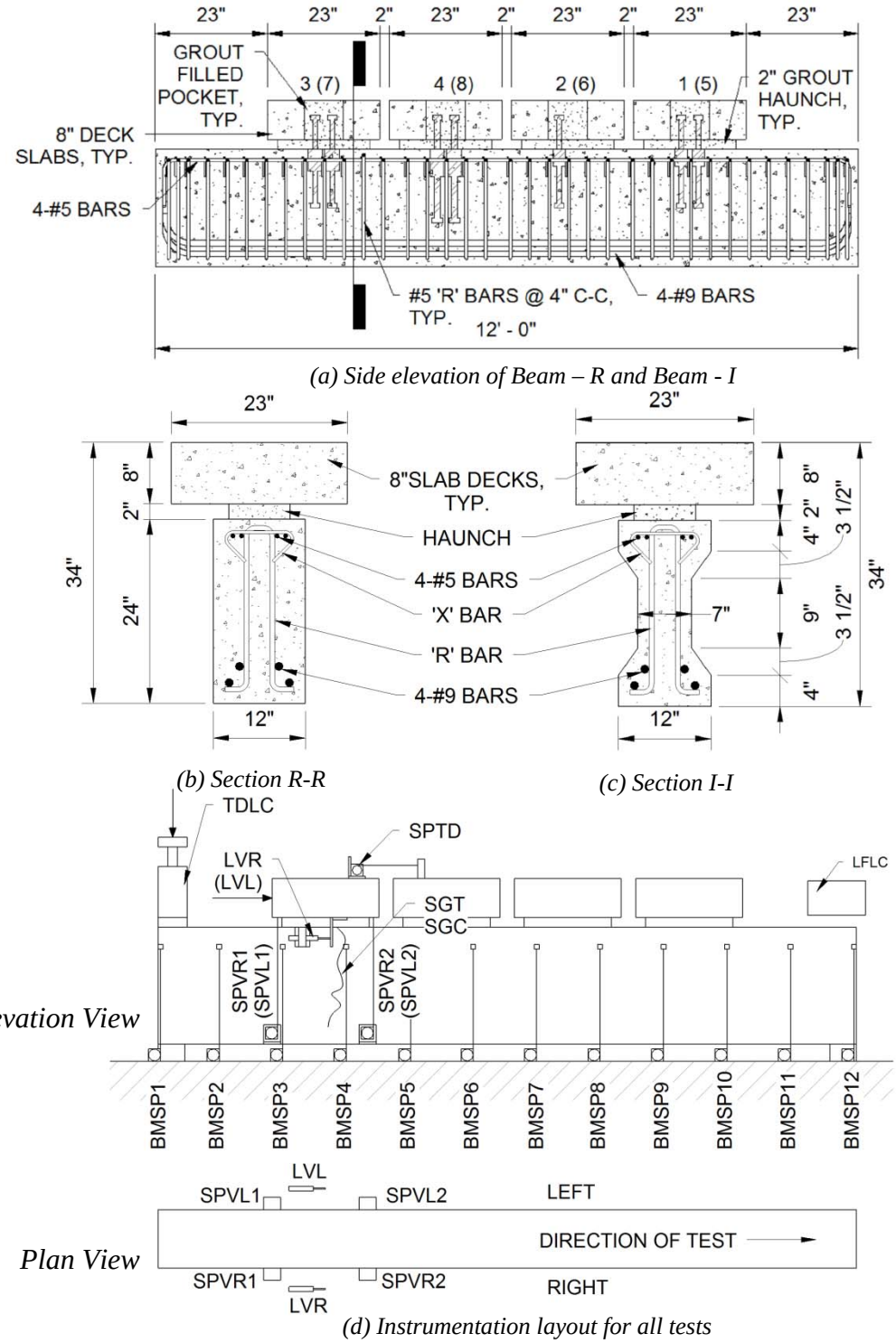

Fig. 7 – Details of experimental specimens. The number given above the slab portions indicate specimen number. Specimens 1 to 4 used section R-R, while Specimens (5) to (8) used section I-I. (1-in. = 25.4 mm).

2.4.2 Instrumentation

Data collection was performed using various types of instruments at key locations on the test setup. An important parameter to capture was the displacement of the deck specimen relative to the test beam it was connected to. A string potentiometer was mounted on the centerline of the specimen to capture its relative displacement while a linear variable differential transducer (LVDT) was mounted on each side of the deck specimen to monitor any twisting in the horizontal plane. String potentiometers were also attached on the underside of the deck specimens at its four corners to monitor uplift. String potentiometers were mounted at 12 in. centers along the test beams to measure the beam deflections as the lateral loads were increased. Half-bridge strain gauges were mounted to one of the connectors of each test to measure the connector strain. A 2000 kip load cell, attached in series to the hydraulic ram, monitored the lateral force. A 60 kip load cell was placed within the tie-down assembly to measure the uplift force at the end of the beam. The notation for the instrumentation shown in Fig. 7d is as follows: SPVRx = string pot-vertical displacement-right side; SPVLx = string pot-vertical displacement-left side; SPTD = string pot-total displacement; BMSPx = string pot-beam-vertical displacement; LVR = LVDT-deck-horizontal displacement-right side; LVL = LVDT-deck-horizontal displacement-left side; SGT = strain gauge-tension side; SGC = strain gauge-compression side; LFLC = load cell-lateral force; TDLC = load cell-tie down force.

2.4.3 Deck segments and connector details

Fig. 8 presents details for deck and connector specimens. The deck specimens consisted of a nominal 23" x 23" x 8" slab with a 10" x 7" pocket that was blocked out during casting. The reinforcing details for the slab included a top layer of #4 bars and a bottom layer of #3 bars in the longitudinal direction, and a top layer of #5 bars with a bottom layer of #4 bars in the transverse direction. All deck segments were each poured at the same time from the same mix of concrete that had a target strength of 5000 psi.

The connectors for each test specimen were varied by size and type. The connectors were cut from lengths of either threaded rod or coil rod. Each connector specimen was cut into two pieces and then threaded together with a coupler during the assembly process. The bottom portion, which was cast into the beam along with the coupler, had a varying length based on the size of the connector. The embedment length was taken to be 12 times the nominal connector diameter. The top portion of the connector was cut in order to place the top of the connector 7-in above the top of the beam. This cut length varied depending on the coupler depth for each connector specimen. Nuts were placed on each end of the connector specimens in order to improve the anchorage of the connector. The threaded rod and coil rod specimens had material designations of B7 and B12, respectively. The specified and measured material properties for the connectors are listed in Table 1 and stress-strain plots are presented in Fig. 9.

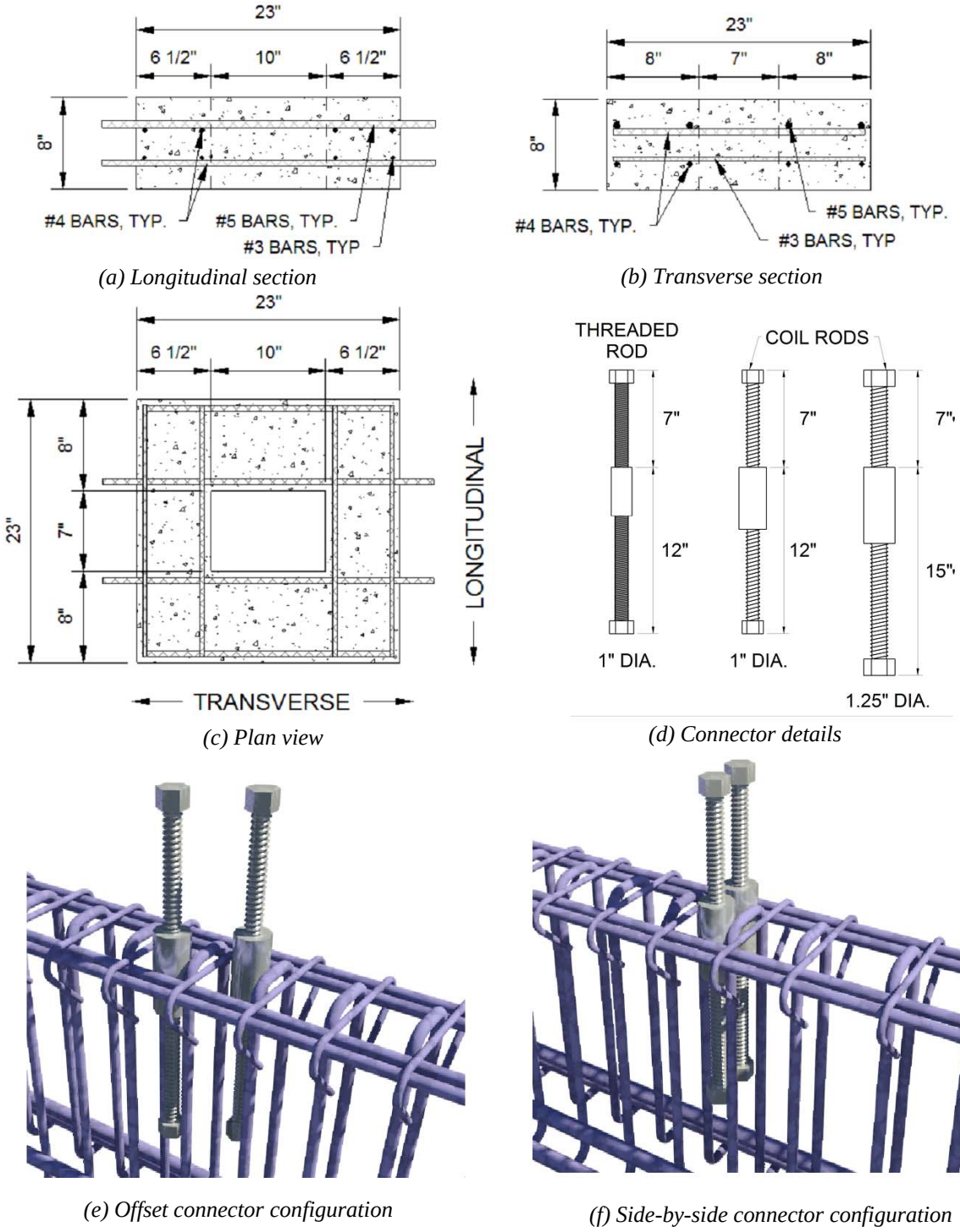

(a) Longitudinal section

(b) Transverse section

(c) Plan view

(d) Connector details

(e) Offset connector configuration

(f) Side-by-side connector configuration

Fig. 8 – Reinforcing details for deck specimens and details for connector specimens. (1 in. = 25.4 mm).

Table 1 – Shear test matrix.

Specimen	Connector Details						Beam Type	Test Name*
	Connector Type	Connector Diameter (in)	Strength					
			Specified Yield, (ksi)	Tested Yield, (ksi)	Specified Tensile, (ksi)	Tested Tensile, (ksi)		
1	TR	1.0	105	131	125	141	R	1-in. TR-R1
2	TRH	1.0	105	131	125	141	R	1-in. TRH-R2
3	CR	1.0	120	100	140	134	R	1-in. CR-R3
4	CR	1.25	105	120	123	135	R	1.25-in. CR-R4
5	CR	1.0	120	100	140	134	I	1-in. CR-I1
6	TR	1.0	105	131	125	141	I	1-in. TR-I1
7	CR	1.0	105	120	123	134	I	1-in. CR-I3
8	CR	1.25	105	120	123	125	I	1.2-in. CR-I4

*Notation used in Test Name

1 in or 1.25 in = Nominal diameter
TR = Threaded rod
TRH = Threaded rod with side-by-side configuration
CR = Coil rod
Rx or Ix = Beam type and test number for respective beam type

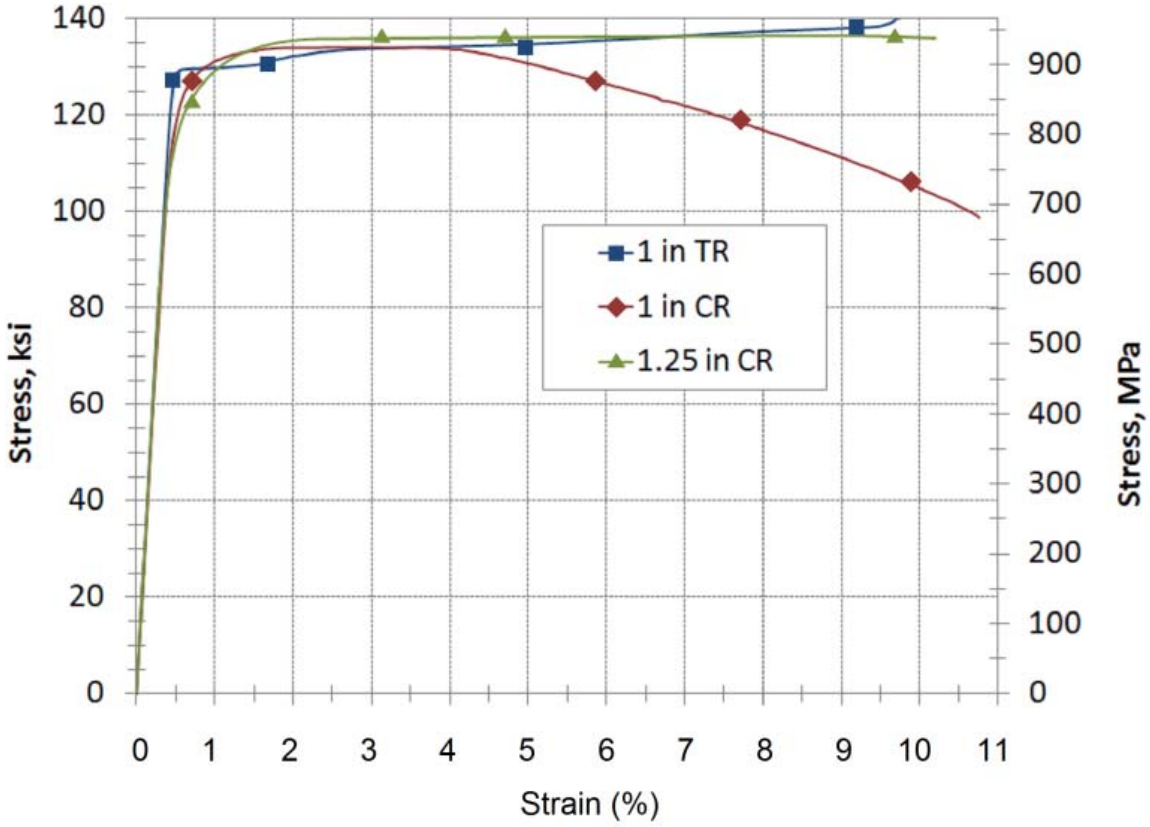

Fig. 9 – Stress-strain plots for shear connector specimens: 1-in. TR, 1-in. CR, 1.25-in. CR.

2.4.4 Materials

Ready mix concrete conforming to TXDOT class "H" 5000 psi mix was used for the beams and deck segments. All concrete elements were poured on the same day and had a measured compressive strength of 6840 psi at time of testing. Grade 60 rebar was used to reinforce the concrete elements including all #3, #4, #5 and #9 bars. Measured yield strength for the reinforcing bar was 59 ksi.

A proprietary grout mix was used to form the haunch and fill around the connectors in the pockets. Two mixes consisting of the proprietary grout were used: (i) a water/powder (w/p) mix of w/p = 0.19 was used to form the haunch and the bottom portion of the pocket; and (ii) a w/p = 0.16 was used to fill the remainder of the pocket. The haunch grout was poured and approximately 6 hours later, when initial set was reached, the pocket grout was mixed and placed. Standard 2-in grout cubes were tested to verify strengths. Compressive grout strengths at the time of push-off testing were 8730 psi and 9510 psi for the haunch and pocket locations, respectively.

2.4.5 Experimental setup

Details for the experimental setup are shown in Fig. 10. The experimental setup made use of a reaction frame previously used in the laboratory. A 600 kip hydraulic actuator was placed to apply the main lateral force to the specimens via W14x109 spreader beams and high-strength thread bar. One end of each test beam was bearing on the reaction frame through wood blocks while the other end was anchored to the laboratory floor to resist uplift forces. A 2000 kip load cell was placed on the hydraulic actuator to

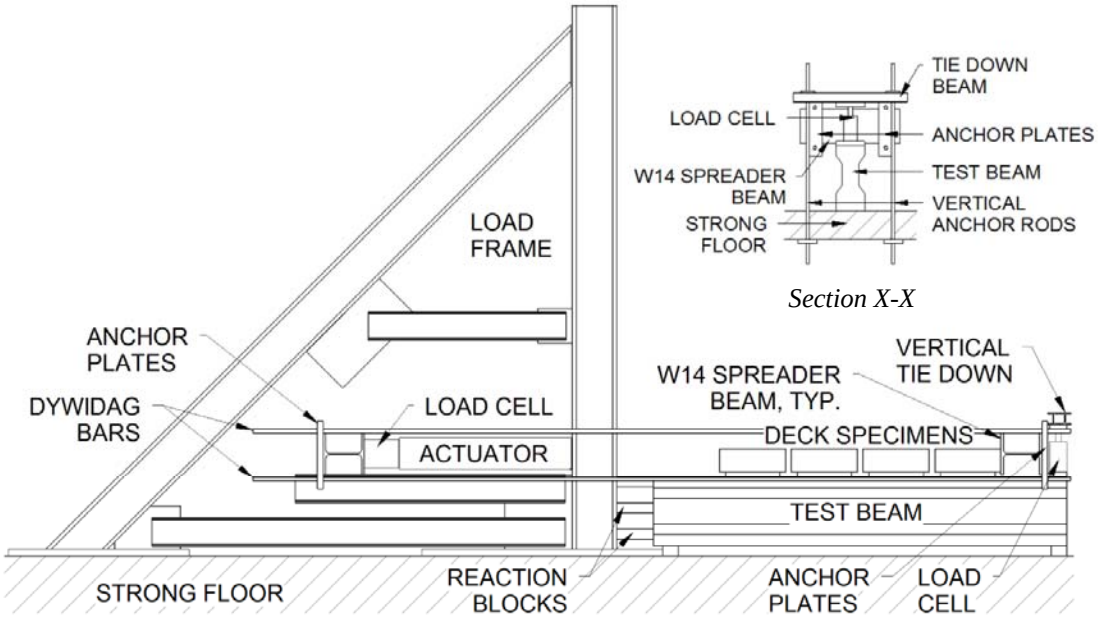

Section X-X

(a) Elevation view

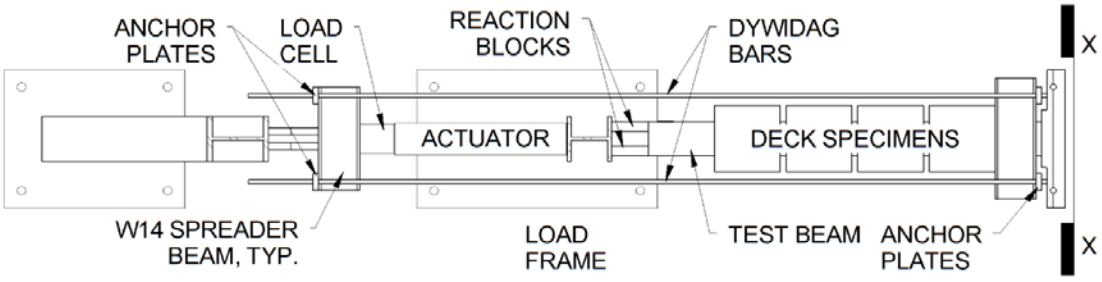

(b) Plan view

Fig. 10 – Experimental test setup schematic.

measure the lateral force, and a 60-kip load cell was placed on the end of the test beam to measure the uplift force.

2.5 Experimental Plan

Tests on the eight specimens were performed to investigate the effects of connector type and size, and beam geometry on the overall girder-pocket-haunch connection. Four test specimens were fastened by shear connectors onto a reinforced concrete beam with a rectangular cross-section, while the other four specimens were fastened to a beam with an I-shaped cross-section. The intent of the latter was to investigate the effect, if any, of a narrow web width on connector performance.

Three types of connectors were used that included: 1-in. diameter threaded rod: 1-in. diameter coil rod: and 1.25-in. diameter coil rod. The threaded rod connectors were used in the rectangular beam to compare with Henley's (2009) test results and also to evaluate their performance in an I-shaped girder. The coil rods were used as a relatively inexpensive alternative to a more costly threaded rod with coupler connector. The 1.25-in. coil rods were used to observe the effects of using large connectors in a constructed pocket space along with a narrow-webbed beam.

Tests were performed on the rectangular beam to evaluate characteristics of the threaded and coil rod while tests on the I-shaped girder were performed to monitor any effects the narrow web may have on the deck-girder connection. A test matrix was created to organize the 8 test specimens. The specimen nomenclature was based on the

type of connector tested, connector size and its position in the test sequence for a given beam type and is shown in the shear test matrix given in Table 1.

2.5.1 Experimental procedure

The following procedure was followed from start of fabrication throughout the testing of each specimen:

1. Cast test beams and deck specimens.
2. Assembled deck-to-girder connection by installing upper portion of connectors and pouring grout haunch/pocket (four deck specimens per beam).
3. Fabricated mounts for all instruments and attached to specimens.
4. Placed rectangular beam in testing location.
5. Assembled the spreader beams, tie rods, tie-down assembly, and instrumentation.
6. Elevated spreader beams with jacks to give approximately 0.25-in. clearance with the test beam/load frame.
7. Began loading the specimen, at approximately 10 kips, released jacks from spreader beams.
8. Allowed loading to continue at 0.003 in/s until connection failure or an acceptable displacement limit was reached.
9. Released the load on the actuator, replaced the jacks under spreader beams to stabilize, and removed tested deck specimen.
10. Moved the spreader beam to the next deck specimen location, repeated steps 5-9.
11. After second test on rectangular beam was completed, tie-down assembly, spreader beam, and tie rods was removed.

12. Removed rectangular beam, rotated 180°, and replaced in testing location.
13. Repeated steps 5-10 for remaining specimens on rectangular beam.
14. Removed rectangular beam and replaced with the I-beam.
15. Repeated steps 5-11 for the I-beam.

2.6 Experimental Results

Results from the eight laboratory experiments are presented in Figs. 11 through 16 and used to characterize performance characteristics of the pocket-connector-haunch system.

Fig. 11 presents the overall lateral force-displacement data for each specimen in an unscaled form. Fig. 12 gives plots of strain-displacement obtained from the half-bridge strain gauges attached to the connectors. Data from the strain gauges was valid only to a certain point as the gauges were damaged and broke away from the connectors. An alternate method of inferring connector strain is shown in Fig. 13.

The inferred strain data was gathered by averaging deck uplift measured by the four string pots mounted to the underside of the deck specimens (SPVxx, refer to Fig. 7), and dividing by the original length of the connector specimen. The inferred strain is given by:

$$\varepsilon = \frac{\delta_{sp}}{L_o} \tag{2}$$

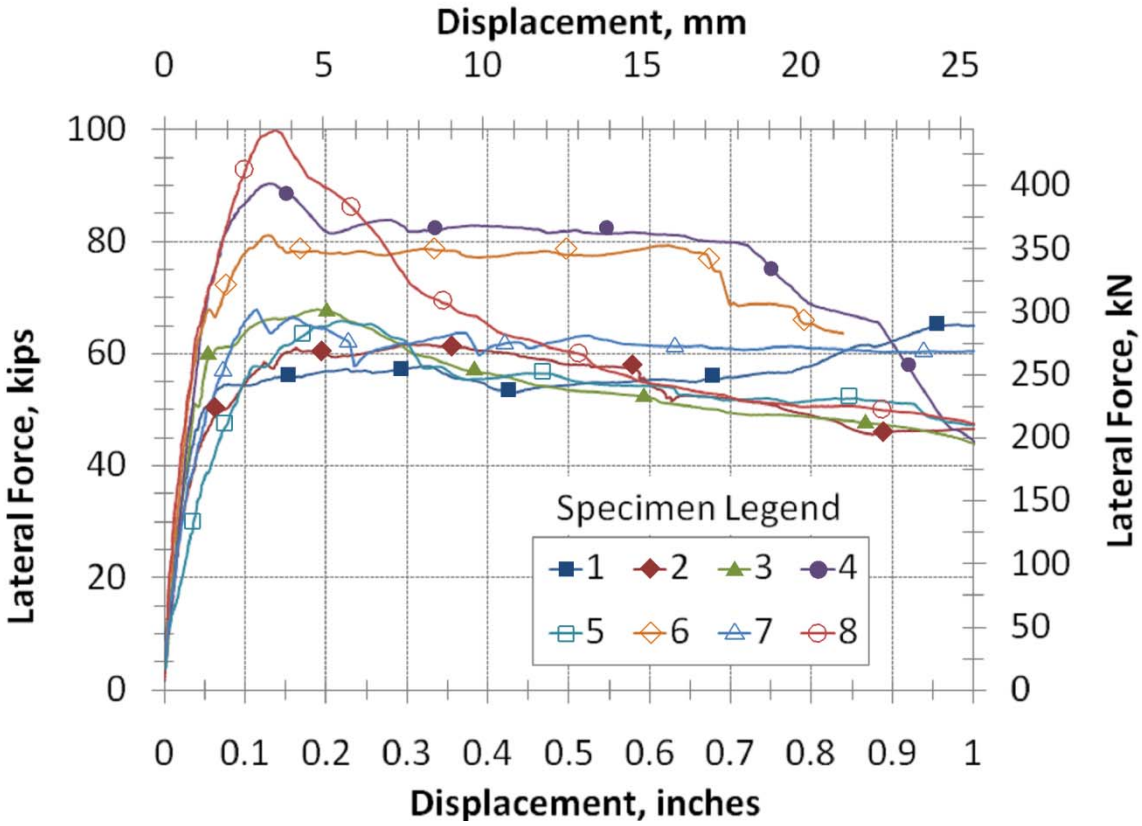

Fig. 11 – Unscaled results for all specimens.

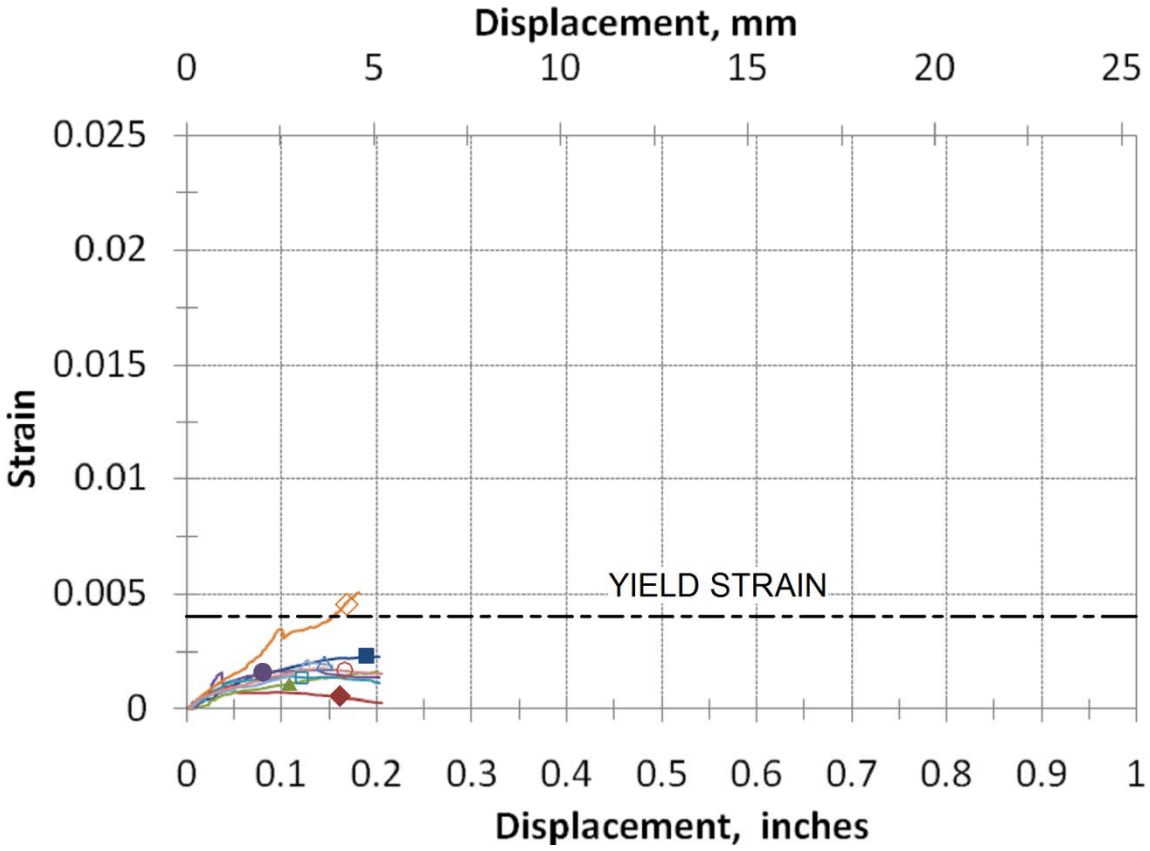

Fig. 12 – Strain gauge results.

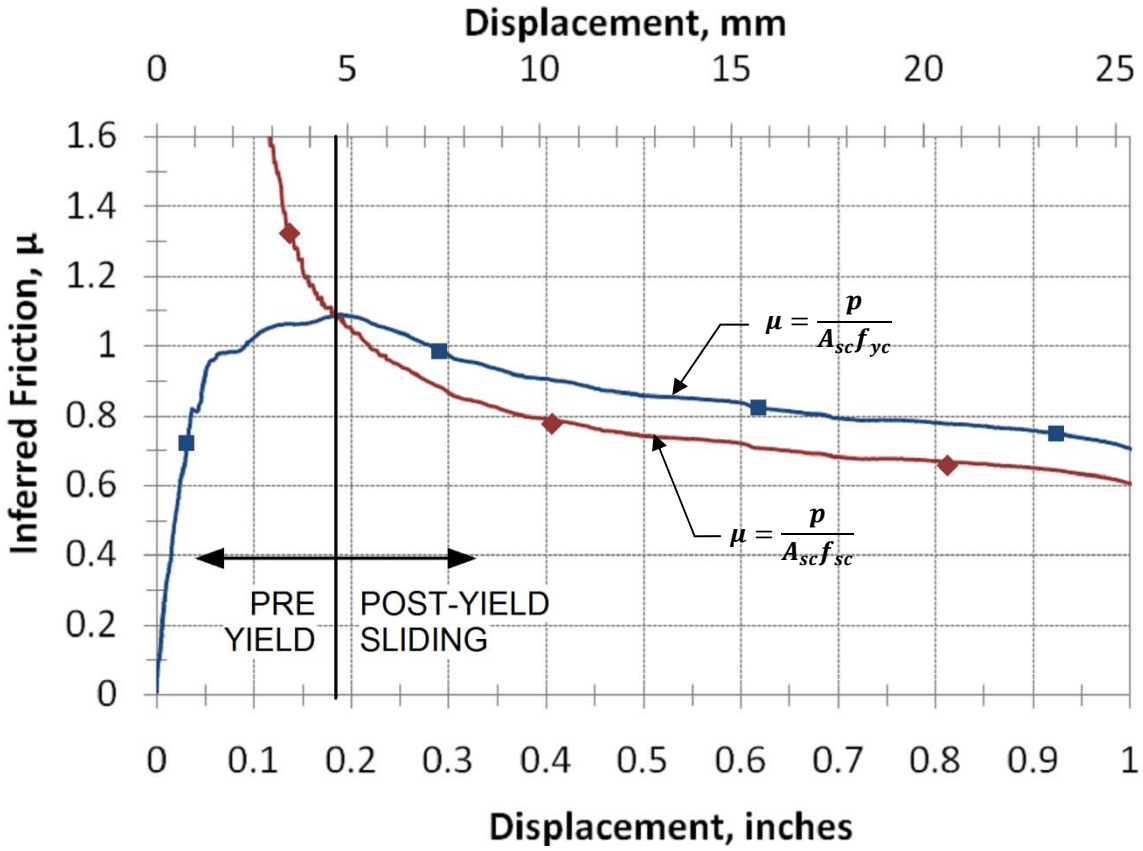

Fig. 13 – Friction inferred two ways for Specimen 3.

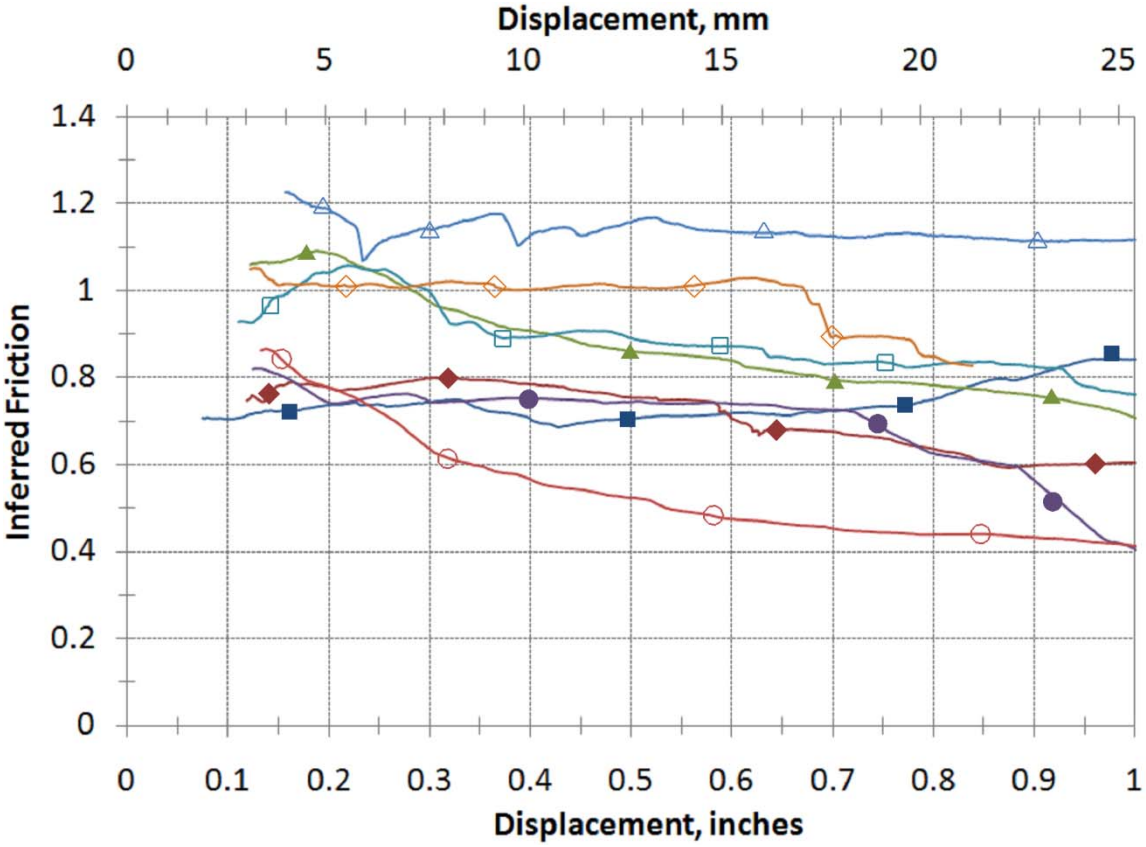

Fig. 14 – Inferred Friction.

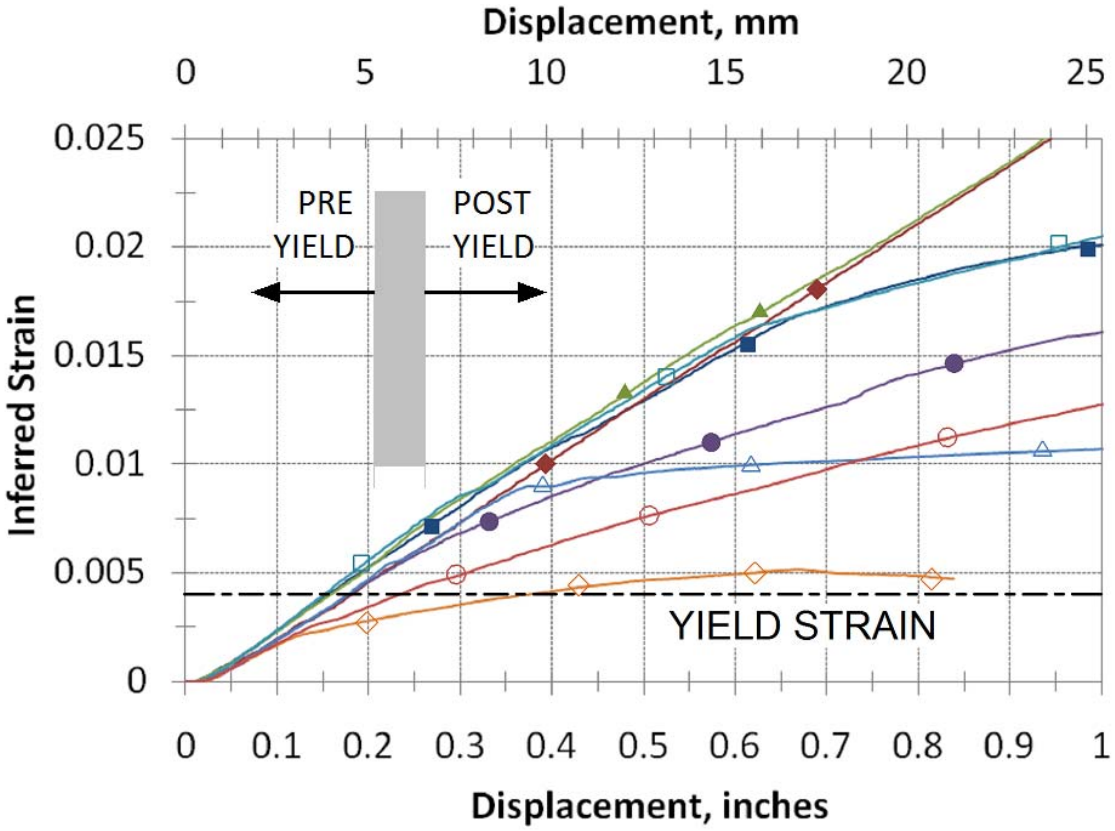

Fig. 15 – Inferred overall bolt strain.

Fig. 16 – Photo of crack angle in Specimen 3.

where ε = the inferred strain; δ_{sp} = the average of the four string pots; and L_o = the original length of the connectors.

As the lateral load on the specimen increased, the initial adhesive bond broke which quickly led to yielding of the connector. The connector yield force effectively clamped the precast concrete deck specimen to the girder which in turn provided lateral resistance via sliding friction. Fig. 14 shows the friction coefficient inferred for Specimen 3 calculated in two ways:

$$\mu = \frac{P}{A_{sc} f_{yc}} \tag{3}$$

where A_{sc} = cross-sectional area of the shear connector; and f_{yc} = connector yield stress and,

$$\mu = \frac{P}{A_{sc} f_{sc}} \tag{4}$$

where f_{sc} = the actual stress in the connector inferred from the strain and the stress-strain behavior in Fig. 9.

The intersection of the two plots in Fig. 14 reveals the point at which the connector evidently yielded. This point also marks the transition from pre-yield loading to post-yield sliding, where all previous adhesive bond is lost. This result corresponds well with inferred strain data in Fig. 13.

Fig. 15 presents the inferred friction-displacement plots for each specimen beyond their initial peak. The force resultant of the vertical-tie down force with the lateral load makes an angle with a vertical reference plane equal to the friction angle, φ, where $\mu = tan\varphi$. Fig. 16 shows a photo of Specimen 3 that has two clearly open cracks formed at an angle of approximately 47° from vertical, implying μ = 1.07. This result

agrees well with the observed friction coefficient at 0.2-in. as seen in Fig 14. Note that the crack first formed just prior to this displacement when the peak load occurred.

2.7 Discussion

From the inferred friction results presented in Fig. 15, it is evident that the coefficient of friction decreases as displacements increase. This is not surprising as the crack interface asperities become abraded and polished as the displacement amplitude increases. The inability to sustain high friction coefficients at large displacements appears to be due to the grout material being devoid of large aggregate. However, it is also evident that there is significant randomness in the observed results. Specimens 6 and 7, in particular, exhibited a consistently high friction coefficient following the initial peak.

The American Concrete Institute Building Code Requirements for Structural Concrete (ACI Committee 318 2008), allow for shear friction capacity to be calculated by:

$$V_n = A_{vf} f_y \mu \tag{5}$$

where μ = 0.6 for concrete placed against hardened concrete not intentionally roughened. However, given that the expected sliding displacement for field applications should be less than 0.25-in, it is evident from Fig. 15 that a dependable friction coefficient of μ = 0.8 may be used in conjunction with the usual undercapacity factor for shear $(\phi = 0.75)$ for design. It should be emphasized, however, that this recommendation is for a deck-grout-girder *system*, where the interfaces are not

intentionally roughened. As suggested by ACI 318-08 and AASHTO, higher friction coefficients may be expected with roughened surfaces. However, more tests should be conducted with material other than grout to investigate whether the presence of a coarse aggregate may also improve performance.

During testing, it was noted that pocket grout tended to crumble quite extensively as the lateral displacement amplitude increased. However, for Specimens 6 and 7, the grout did not show extensive damage. Pocket grout for Specimens 6 and 7 was significantly harder than grout from other specimens. An air chisel was required to break grout away from the pocket in order to remove the deck specimens after testing. Grout in these two specimens was strong enough to resist forces from the connector that led to minimized deck uplift. This is evident in the inferred strain plots for Specimens 6 and 7 in Fig. 13. The plots for these specimens have a distinct plateau over the other specimens. As damage increases in the pocket grout, the connector can no longer maintain load and the deck begins to displace more, which is evident by an increasing inferred strain-displacement plot and a decreasing inferred friction-displacement plot.

Samples of grout from Specimen 6 were salvaged and tested. Secondary tests on two grout cubes taken from Specimen 6 had compressive strengths of 5.3 ksi and 5.6 ksi. These are well below the average compressive strengths observed the testing of other cubes. It cannot be strictly concluded from the information obtained for these two specimens that a sufficiently strong grout is the sole contributor to a better performing connection evident by a constant post-peak coefficient of friction, although physical evidence observed at time of testing tended to lean towards a stronger grout. Figs. 17

and 18 show photos of tested specimens, notably the condition of the grout elements. The specimens in Fig. 17 showed typical grout failures including extensive damage and a clear location were the connector bolts pulled away from the grouted pocket. Fig. 18 shows photos of the grouted pockets of Specimens 6 and 7. The grout in these pockets did not display the same level of damage as in other specimens. Fig. 18(a) shows a connector still anchored to the grout after testing.

The performance of the I-shaped test beam proved to be adequate compared to that of the rectangular test beam—no adverse effects were observed due to the narrow web of the I-shape. One concern with the I-shaped section is the ability to place the connectors within the beam web space along with the required beam reinforcement. The relatively narrow web geometry of an I-shaped section can make this a difficult task. With the constrained dimensions on the I-shaped test beam, the connectors were placed in a staggered fashion without issue, including the larger 1.25-in. anchorage shown in Fig. 8.

Specimen 8 showed the highest peak strength capacity (100 kips). But it appears that this large force was instrumental in precipitating a partial pull-out of the grout within the pocket and led to a steady decline in the resistance. The nut head at the top of each threaded rod connector extended into the deck to an elevation just below the top

(a)

(b)

Fig. 17 – Photos of typical grout failures.

(a)

(b)

Fig. 18 – Photos of strong grout in Specimens 6 and 7.

layer of deck reinforcement. This may have negated engagement of the top layer of deck steel in providing pocket-grout pull-out resistance. The downward load path from the bolt head led to the bottom layer of deck reinforcement and subsequently formed a horizontal failure plane containing the lower steel layer. In an attempt to alleviate this detailing issue, the top of the connectors should be placed as high in the deck as practicable to improve the anchorage mechanism of the bolts. Additional washers may also be used to increase connector bolt anchorage. Roughening the pocket walls may also increase the bond between the grout and concrete to improve the transfer of force between the two.

Full-depth precast panels can be used in bridge structures to provide a method for rapid deck construction method. A key element in the full-depth panel system is the shear connection between the girder and the deck panel. This connection will greatly affect the level of composite action that can be achieved between the girder and deck.

Eight single-pocket deck segments were “pushed-off” to examine the horizontal shear-displacement performance of the deck-to-girder connection, where threaded and coil rods were tested on an I-shaped test beam to monitor effects of a narrow web (coil rod connectors were tested as a possible lower cost alternative to threaded rods). Initial failure of the adhesive bond between the haunch and girder led to a sliding mechanism for the deck segments. This sliding mechanism then led to yielding of the connectors and in turn provided a clamping force from which a consistent sliding coefficient of friction was observed. The ability of this clamping force to be sustained throughout increasing displacements is dependent on the pocket grout strength. If the grout strength

is sufficiently strong to inhibit other failure modes such as cone pull-out within the deck, a constant coefficient of friction is observed to occur after the initial peak. If the grout does not have sufficient strength, connector anchorage in the pocket grout degrades leading to a decreased resistance.

The tests included connector specimens of threaded rod that were tested to give a common point of reference with experiments done by Henley (2009). Henley's tests on threaded rods with couplers with a 2-in. haunch showed similar behavior to threaded rod specimens in this research. Threaded rod specimens with couplers in Henley's experiments had sustained friction coefficients of about 0.6 and 0.7. Threaded rod specimens in this research showed friction coefficients in the range of 0.7 to 1.0. The friction coefficient plots in Henley's experiments did not contain a distinct decline as displacement increased as was evident in this research.

In order for the connector system to be viable, it is key to have sufficient stirrups in the local area of the shear connectors, which will allow the high pull-out force to be resisted and prevent premature damage the girder. The amount of shear steel was increased from Henley's tests and no brittle premature beam failures were encountered.

2.8 Closure

Based on the experimental study presented herein, the following key findings and conclusions are drawn.

1. A *systematic* experimental setup is needed to properly evaluate the performance and interaction of a deck-haunch-girder system, most notably at an ultimate limit state.
2. Although connector placement is more difficult due to reinforcing cage congestion the narrow-webbed I-girder shape showed no detrimental behavior as compared to the full rectangular beam section.
3. Closely spaced hoops in the vicinity of the connectors are necessary to ensure an effective non-contact splice. Sufficient hoop steel will allow the girder, notably the narrow-webbed girders, to carry the high pull-out forces from the connectors.
4. The lateral load capacity of the connectors is directly dependent on the net area of steel in the connection rather than the type of threads on the connector.
5. An average of μ = 0.85 in the displacement range of 0.25 to 0.5-in. was observed. However due to variability, a dependable value of μ = 0.8 used with the undercapacity factor ($\phi = 0.75$) is recommended for design of grout placed against hardened concrete not intentionally roughened.
6. Coil rod specimens showed similar behavior when compared to the threaded rod specimens. This demonstrates prestressed concrete based hardware that typically uses coarse threads (such as the coil rod thread bar used in this study), and is somewhat less expensive than fine thread threaded rod and high-strength bolts, may be used without any sacrifice in performance.
7. The strength of the grout in the pocket has an effect on the nature of the coefficient of friction-lateral displacement of the deck. A strong grout leads to a

relatively constant coefficient of friction, and a weaker grout shows a distinct decline in the coefficient of friction as displacements are increased.

CHAPTER III

DESIGN OF SHEAR CONNECTORS FOR PRECAST CONCRETE BRIDGE DECKS: TRUSS MODELING APPROACH

3.1 Chapter Summary

The successful implementation of a full-depth precast deck-panel system requires the use of a viable design methodology that properly accounts for *system* behavior including the fastening of the precast deck panels to the prestressed concrete girder. A methodology is presented for the design of a deck-haunch-girder connector-in-pocket system using a truss modeling approach. Such an approach is necessary because substantial cracking is expected at the deck-haunch interface at an ultimate limit state; traditional shear/beam theory does not account for the decreased ability of shear stresses to transfer across open cracks. Design solutions are presented utilizing the Rock Creek Bridge in Parker County, Texas as an example structure.

3.2 Background Information and Scope

In analyzing the interface shear stresses for a cast-in-situ slab-on-prestressed precast concrete girder bridge, one would normally use customary beam theory assuming uncracked sections. This leads to the well-known equation for shear stresses in a homogeneous beam:

$$\tau = \frac{VA\bar{y}}{Ib} \tag{6}$$

where $V =$ applied shear force; $A\bar{y} =$ statical first moment of the area above shear interface, about the neutral axis; $I =$ second moment of area of section; and $b =$ width of section at point of interest. However, in the ultimate limit state, even though a slab-on-girder bridge may be prestressed, in positive moment regions it is inevitable that the cracks pass the flange-web interface violating the assumptions implicit in the well known shear stress formula. Instead a truss-like stress field develops as the neutral axis moves up into the deck/flange.

This issue becomes even more problematic when dealing with precast deck segments that have discrete deck-to-girder connectors. that are significantly more widely spaced than normal transverse hoop (shear) reinforcement.

Due to the fact that concrete members are inevitably cracked at an ultimate limit state, a design method that realizes and accounts for this cracking is needed for a concrete system such as a full-depth precast deck-on-girder system. One such method of design, that is adopted herein, is a truss model. Kim and Mander (2007) developed continuum and discrete truss models that implicitly account for shear and flexure effects. Based on minimization of energy in the shear and flexure mechanisms, a diagonal crack angle, θ, was determined.

This chapter adapts the Kim and Mander (2007) truss models that were previously developed for beam-columns, to prestressed concrete beams that account for both the so-called B and D-regions (where B = Beam and D = Disturbed regions).

This chapter first examines the formulation of the two main mechanisms that lead to failure in a bridge constructed with precast deck panels-on-precast prestressed

concrete girders. These are (i) sliding shear between the deck panels and girder; (ii) web shear in the precast prestressed girders. A four-step design methodology is then proposed. The chapter concludes with a design example based on the Rock Creek Bridge in Parker County, Texas.

3.3 Sliding Shear Strength

The shear connectors used in a full-depth precast deck-panel system effectively extend the transverse reinforcement of the girder into the deck by forming a non-contact splice. From the experimental investigation of Chapter II, a system of this nature has an associated coefficient of friction, μ, in the range of 0.8 ($\pm$20%). This value is a measure of the horizontal resistance provided by the shear connectors, and is used in the derivation of the sliding shear resistance of a full-depth precast panel.

Fig. 19 shows a free-body diagram of a deck-haunch-girder segment with key components labeled. The horizontal resistance to sliding shear in the interface between the deck and girder is provided by friction induced from the yield force of the connector. Over one panel length, the shear resistance can be calculated from:

$$V = \frac{dM}{dx} = jd_o \frac{dC}{dx} = jd_o \frac{\Delta C}{\Delta x} = \Delta C \frac{jd_o}{L_{panel}} \tag{7}$$

in which $jd_o =$ internal lever arm from top compression chord to bottom tension chord of truss; $L_{panel} =$ panel length and:

$$\Delta C = \mu N_p A_{sc} f_{yc} \tag{8}$$

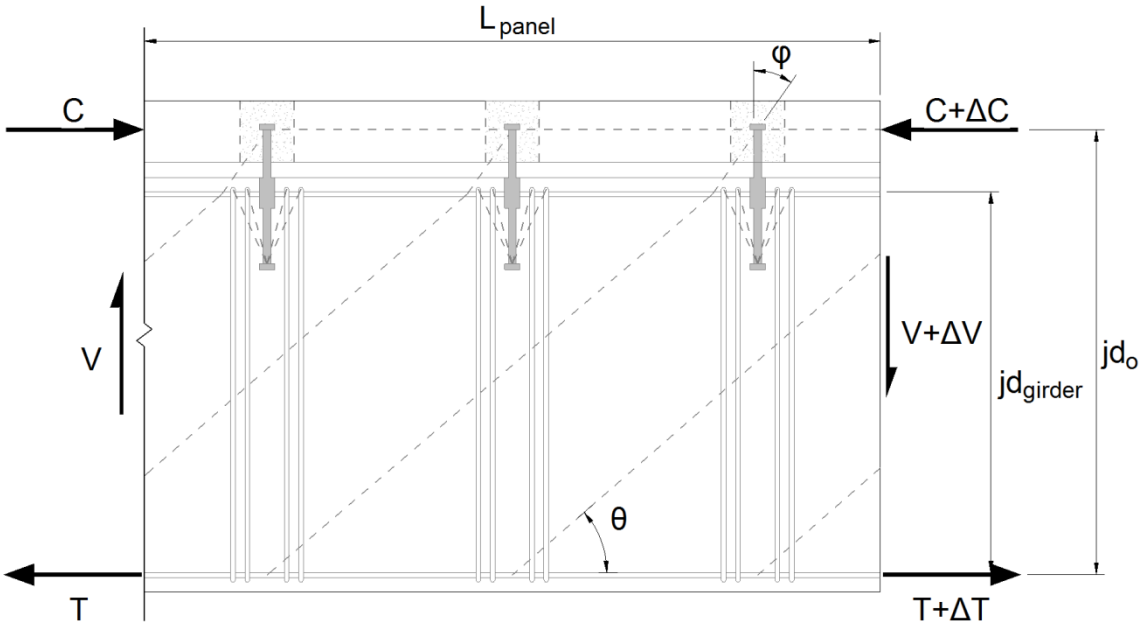

Fig. 19 – Free-body diagram of panel and girder segment.

where $\mu =$ coefficient of friction; $N_p =$ number of pockets in a panel; $A_{sc} =$ total area of shear connector steel in a pocket (sum of the root thread areas); and $f_{yc} =$ yield strength of the shear connectors.

Pocket spacing, s_p for the pockets, is set based on the number of pockets and is given by:

$$s_p = \frac{L_{panel}}{N_p} \tag{9}$$

where $L_{panel} =$ the length of the precast deck-panel.

To maintain equilibrium over one panel length, the increase in the bottom chord (ΔT) force must be equal to the top chord force (ΔC). The top and bottom chords of the overall truss create a force couple, leading to a resisting moment increase (ΔM) given by:

$$\Delta M = \mu N_p A_{sc} f_{yc} j d_o \tag{10}$$

Thus the sliding shear capacity for an individual panel is found by dividing (10) by the panel length:

$$\phi V_{slide} = \phi \mu N_p A_{sc} f_{yc} \frac{j d_o}{L_{panel}} \tag{11}$$

to give the dependable shear resistance provided by the shear connectors in one pocket. (11) allows N_p to be determined such that $\phi V_{panel} \geq V_u - \phi V_p$ where $V_u =$ applied factored shear force and $\phi V_p =$ shear carried by the inclined component of the prestress, if any, thus $V^* =$ net shear force (demand) to be carried by the connectors.

3.4 Non-contact Splice

In order for the shear connectors to develop their full tensile strength when anchored within the girder a non-contact splice must be formed to complete the tension tie of the truss (see Fig. 19). Thus, the number of transverse hoops in the group (N_{group}) that are needed to resist the tensile load of the shear connector can be determined by:

$$N_{group}A_{sh}f_{yh} > A_{sc}f_{yc} \tag{12}$$

where A_{sh} and f_{yh} are the cross-sectional area and yield strength of a single hoopset, respectively.

Fig. 20 shows the transverse hoops required to anchor the shear connector placed within $0.5h_{ef}$ either side of the shear connector, as recommended in Henley (2009) and Appendix D of ACI 318 (2008), where h_{ef} = effective embedment depth, to the top of the bottom nut, of the shear connector. This detailing aspect is key to developing a system with a ductile failure mechanism as opposed to a brittle failure.

3.5 Web Shear Strength

A proper design method for the full-depth precast deck-panels will design the shear connectors to resist a sliding shear mechanism, but should also properly design the transverse girder reinforcement to have a sufficient dependable capacity (ϕV_s) to resist the net shear force within the girder itself, thus:

$$\phi V_s \geq V^* = V_u - \phi V_p \tag{13}$$

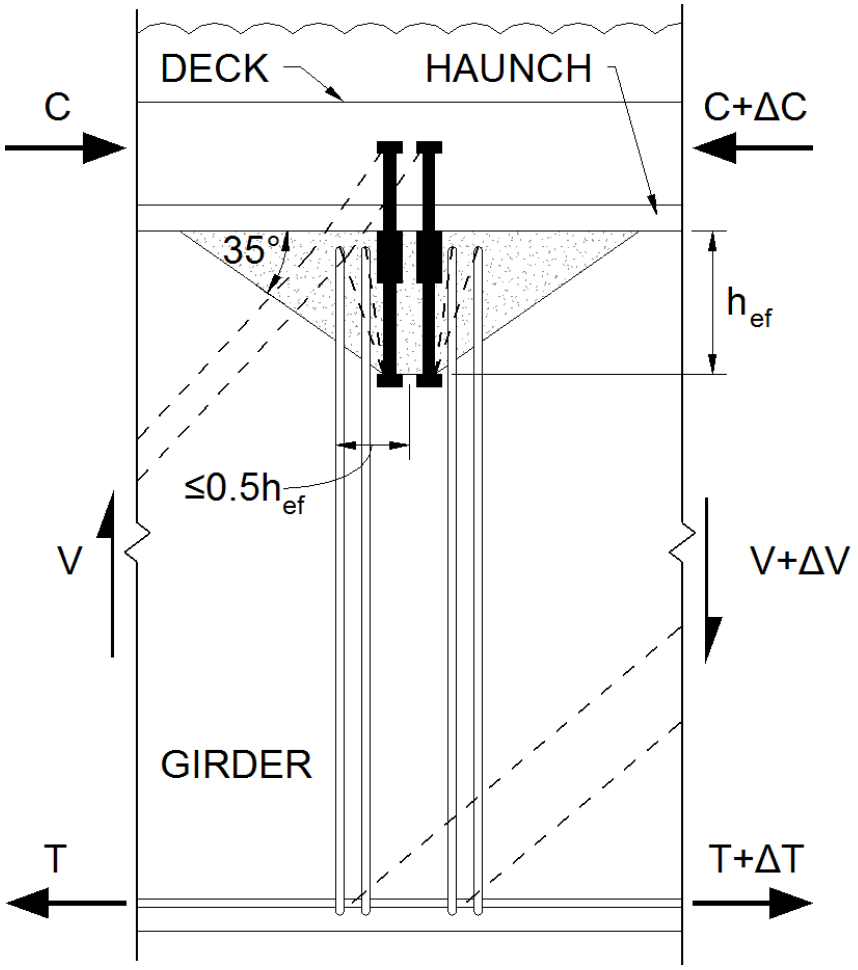

Fig. 20 – Details of non-contact splice.

The shear capacity of the transverse hoops of a truss from Kim and Mander (2005) is:

$$V_s = A_{sh} f_{yh} \frac{jd}{s} \cot\theta \tag{14}$$

where A_{sh} = area of transverse steel in a hoop, f_{yh} = yield strength of the hoop, jd = internal lever arm between the tension and compression chords of the truss within the girder, s = hoop spacing, and θ = inclined crack angle to the longitudinal axis. The term $\frac{jd}{s}\cot\theta$ from (14), is equal to the number of spaces crossed by a crack at an angle θ. Kim and Mander (2007) derived a formulation of this crack angle in beam-column elements using a minimization of energy approach yielding:

$$\theta = tan^{-1}\left(\frac{\left(\frac{\rho_v}{\rho_t}\right)\left(\frac{A_v}{A_g}\right)}{0.61\Lambda}\right)^{\frac{1}{4}} \tag{15}$$

where ρ_v and ρ_t are the volumetric ratios of transverse steel and longitudinal steel, respectively; A_v and A_g are the shear area and gross area of the concrete section, respectively; and Λ = an end-fixity parameter: $\Lambda = 1$ for fixed-pinned and $\Lambda = 2$ for fixed-fixed. This model gives an estimate on the angle at which diagonal struts form in the girder and therefore how many hoopsets are engaged over an inclined crack.

A constructed full-depth precast deck-panel system will not have continuous shear connections, but rather at discrete points, some of which may be widely spaced and requires that discrete geometry be accounted for. Therefore, principles discussed in

Kim and Mander (2005) are built upon to formulate the shear resistance of a full-depth precast deck-panel system.

The following terms of (15) are defined based on girder properties to give:

$$\rho_v = \frac{A_{sh} N_{group}}{b_w s_p} \tag{16}$$

where $A_{sh}N_{group}$ = the total area of transverse hoopsets immediately surrounding the shear connectors in each pocket, b_w = the girder web width, and s_p = the spacing between the pockets. Neglecting the top steel, ρ_t becomes:

$$\rho_t = \frac{2A_{sb}}{A_g} \tag{17}$$

where A_g = gross area of girder; if there is a mix of mild steel rebar (A_s), if any, and prestress tendons, (A_{sp}), the effective area becomes:

$$A_{sb} = A_s + A_{sp}\frac{d_p}{d} \tag{18}$$

where d_p = depth to center-of-gravity of prestress, and d = depth to mild steel reinforcement or center-of-gravity of straight prestress tendons if no mild steel. Note the factor 2 in (17) signifies the steel area in the top and bottom chords are the same.

The shear area term is defined by:

$$A_v = b_w j d_{girder} \tag{19}$$

where jd_{girder} = the internal lever arm of the girder. Substituting (16) through (19) along with $\Lambda = 1$ into (15), the following results:

$$\theta = \tan^{-1} 0.95 \left[N_{group} \frac{A_{sh}}{A_{sb}} N_p \frac{j d_{girder}}{L_{panel}} \right]^{0.25} \tag{20}$$

Substituting (20) into (14) to obtain the final form of ϕV_s gives:

$$\phi V_s = \phi 1.05 N_{group} A_{sh} f_{yh} \left(N_p \frac{jd_{girder}}{L_{panel}} \right) \left(\frac{A_{sb} L_{panel}}{N_{group} A_{sh} N_p jd_{girder}} \right)^{0.25} \quad (21)$$

(21) yields the shear capacity of the transverse girder reinforcement based on the expected crack angle (θ), that develops in a girder under elastic conditions, including service loading, for a given longitudinal and transverse reinforcement layout.

3.6 Steps in the Design Process

The design of a full-depth precast deck-panel will utilize (11), (12) and (21) formulate a constructible solution that resists the applied loading. The key steps in the design of a full-depth deck system are:

1. Determine panel shear demand from applied factored design loads
2. Determine pocket layouts and sliding shear capacity
3. Provide transverse hoops to develop non-contact splice
4. Verify web shear capacity exceeds demand

The goal of the design procedure is to design for sliding shear and verify that the provided transverse reinforcement is sufficient to resist shear in the girder web.

STEP 1: Establish Net Panel Shear Demand

From the applied factored loads and the provided inclined prestress force, determine the net shear demand:

$$V^* = V_u - \phi V_p \quad (22)$$

in which V_u is based on the most adverse combination of factored dead and live plus impact loads, where the dependable shear resisted by the inclined force component of the prestress given by:

$$\phi V_p = \phi F_{ps} \sin \theta_{ps} \tag{23}$$

in which F_{ps} = prestress force in tendons at ultimate; θ_{ps} = angle of inclination of the tendon to the girder axis); and ϕ = undercapacity factor for shear.

STEP 2: Design Pocket Layout and Connectors

Based on the net shear demand, choose a fastener type and number to give A_{sc} and f_{yc}. Then, using (11), determine the number of pockets in a panel such that:

$$N_p \geq \frac{V^*}{\phi \mu A_{sc} f_{yc}} \frac{L_{panel}}{j d_o} \tag{24}$$

STEP 3: Provide Hoops to Form Non-contact Splice

Adopt a hoopset (A_{sh} and f_{yh}) and using (12) determine the number of hoops in a group:

$$N_{group} \geq \frac{A_{sc} f_{yc}}{A_{sh} f_{yh}} \tag{25}$$

STEP 4: Verify Web Shear Capacity Exceeds Demand

Determine the crack angle for the hoops provided from (25) using:

$$\cot \theta = 1.05 \left[\frac{A_{sb}}{N_{group} A_{sh}} \frac{L_{panel}}{N_p j d_{girder}} \right]^{0.25} \tag{26}$$

Hence determine the dependable shear capacity carried by the hoops within the girder web and then check this exceeds the net shear demand (V^*):

$$\phi V_s = \phi N_{group} A_{sh} F_{yh} \frac{N_p j d_{girder}}{L_p} \cot\theta \geq V^* \tag{27}$$

Based on the above equations, Table 2 has been prepared to give some design guidance on the resistance provided by 1-in. and 1.25-in. diameter coil rod for 2 to 7 pockets in an 8-ft. long precast bridge deck panel. Values of Table 1 are calculated using nominal quantities for the coarse-thread coil rod (CR). These include: $A_{s,1\ in.} = 0.54\ in^2$; $A_{s,1.25\ in.} = 0.91\ in^2$; $f_{y,1\ in} = 120\ ksi$; $f_{y,1.25\ in} = 105\ ksi$.

3.7 Design Example: Rock Creek Bridge, Parker County, Texas

3.7.1 Description of bridge

Table 3 gives design data for the Rock Creek Bridge used in this design example. The 120-ft. bridge consists of an 8-in. deck placed on Type IV girders. The girders are prestressed with 58 0.5-in. tendons. The first 4-ft. on either end of the bridge span are cast-in-place, starting the first precast panel at 4-ft. from the bridge ends. The objective of this design example is to use the foregoing theory to design an appropriate connector system for the exterior (fascia) girders.

Table 2 – Panel shear capacities.

	2-1-in. CR		2-1.25-in. CR	
No. Pockets	ϕV_{slide} (kips)	ϕV_s (kips)	ϕV_{slide} (kips)	ϕV_s (kips)
2	94	164	139	223
3	141	223	208	302
4	188	277	278	375
5	235	327	347	443
6	283	375	417	508
7	330	421	486	570

Table 3 – Design data for Rock Creek Bridge.

Name	Value	Comment
L	120 ft	Girder Span
ω_{DL}	1.46 kips/ft	Distributed Dead Load
ω_{LANE}	0.64 kips/ft	Distributed Lane Load
L_{panel}	96 in	Panel Length
jd_o	58 in	Overall Internal Lever Arm
jd_{girder}	49.5 in	Girder Internal Lever Arm
A_{sh}	0.62 in^2	Area of single hoop (#5)
A_{sb}	8.7 in^2	Longitudinal Girder Reinforcement
□	0.75	Shear Reduction Factor
$A_{sc,1\text{-}in.}$	1.08 in^2	Area of 2 1-in. CR
$A_{sc,\ 1.25\text{-}in.}$	1.82 in^2	Area of 2 1.25-in. CR
$f_{yc,\ 1\text{-}in.}$	120 ksi	Yield Strength of 1-in. CR
$f_{yc,\ 1.25\text{-}in.}$	105 ksi	Yield Strength of 1.25-in. CR

3.7.2 Design calculations

Additional calculations not shown here, can be found in Appendix C. Fig. 21 presents the results of the design process carried out for 1-in. CR in all panels.

STEP1: Shear Demand

Based on the loading on the half-span shown in Fig. 21(a), Fig. 21(b) shows the gross and net (demand) shear force diagrams.

The net shear demand at the mid-point of panel 1 is determined to be

$$V^* = 237\ kips$$

Step 2: Number of Required Pockets

Using (24) gives:

$$N_p \geq \frac{V^*}{\phi\mu A_{sc} f_{yc}} \frac{L_{panel}}{jd_o}$$

$$N_p \geq \frac{237kips}{0.75 * 0.8 * 1.08in^2 * 120ksi} * \frac{96in}{58in} = 5.04\ pockets \Rightarrow\ \therefore use\ 6\ pockets$$

$$\phi V_{slide} = \phi\mu N_p A_{sc} F_{yc} \frac{jd_o}{L_p}$$

$$\phi V_{slide} = 0.75 * 0.8 * 6pockets * 1.08in^2 * 120ksi \frac{58in}{96in} = 282kips$$

Step 3: Non-Contact Splice Requirements

Using (25) yields:

$$N_{group} \geq \frac{A_{sc} f_{yc}}{A_{sh} f_{yh}}$$

$$N_{group} \geq \frac{1.08in^2 * 120ksi}{0.62in^2 * 60ksi} = 3.5 \Rightarrow \therefore use\ 4\ hoops/pocket$$

Step 4: Check Web Shear Capacity

Using (26)

$$\cot\theta = 1.05 \left[\frac{A_{sb}}{N_{group} A_{sh}} \frac{L_{panel}}{N_p j d_{girder}} \right]^{0.25}$$

$$(\cot\theta) = 1.05 \left[\frac{8.7in^2}{4 * 0.62in^2} \frac{96in}{6pockets * 49.5in} \right]^{0.25} = 1.08 \Rightarrow \theta = 42.8^{\circ}$$

and

$$\phi V_s = \phi N_{group} A_{sh} f_{yh} \frac{N_p j d_{girder}}{L_{panel}} \cot\theta \geq V^*$$

$$\phi V_s = 0.75 * 4 * 0.62in^2 * 60ksi \frac{6pockets * 49.5in}{96in} (1.08) = 373\ kips \geq V^*$$

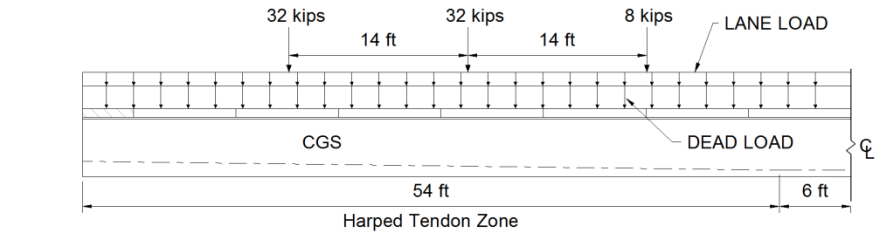

(a) Applied loading

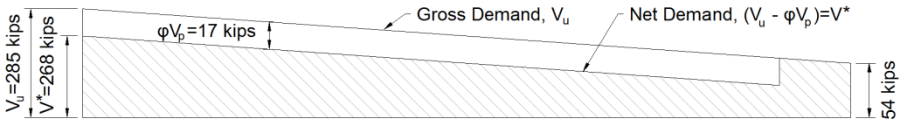

(b) Shear demand

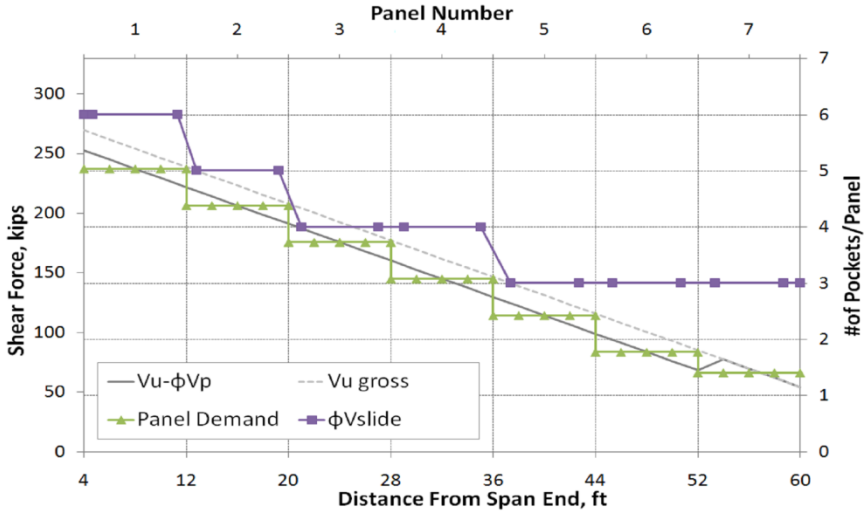

(c) Sliding shear capacity (per panel) vs. demand

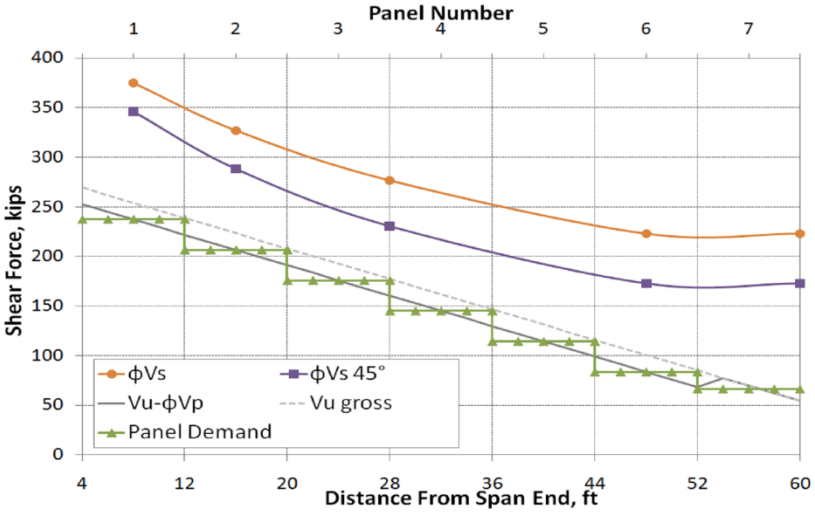

(d) Web shear capacity (per panel) vs. demand

Fig. 21 – Loading demands and capacity diagrams for 1-in. CR connectors.

3.8 Discussion

The design process can be carried out to incorporate various design intents. The solution presented in Fig. 21 is a result of using only 1-in. CR in each panel. As an alternative, 1.25-in. CR can be utilized to arrive at a solution that minimizes differences in the number of pockets per panel. Fig. 22 presents a solution with 1-in. CR and 1.25-in. CR shear connectors showing the sliding shear capacity and the web shear capacity. The design solution shown in Fig. 21 has 5-pocket, 4-pocket and 3-pocket panels. The solution shown in Fig. 22 has only 4-pocket and 3-pocket panel. The manufacturing process can be simplified if a more consistent panel type is used, especially for a long bridge where a large number of panels will be constructed. However, this may require different diameter shear connectors to be provided for the site works. Perhaps an optimal solution is to present several design solution alternative to be constructed; the general contractor will thus select the most practicable solution based on price and construction expediency.

In order for the full-depth precast deck-panel system to remain viable throughout a range of loading, the shear connectors must remain adequately anchored in the girder. A brittle failure can occur if there is not sufficient transverse reinforcement in the area of the shear connectors to develop a non-contact splice.

A consequence of developing the non-contact splice is an increase in transverse reinforcement compared to what would be required by implementing a traditional method of deck construction. However, this increase in transverse reinforcement is

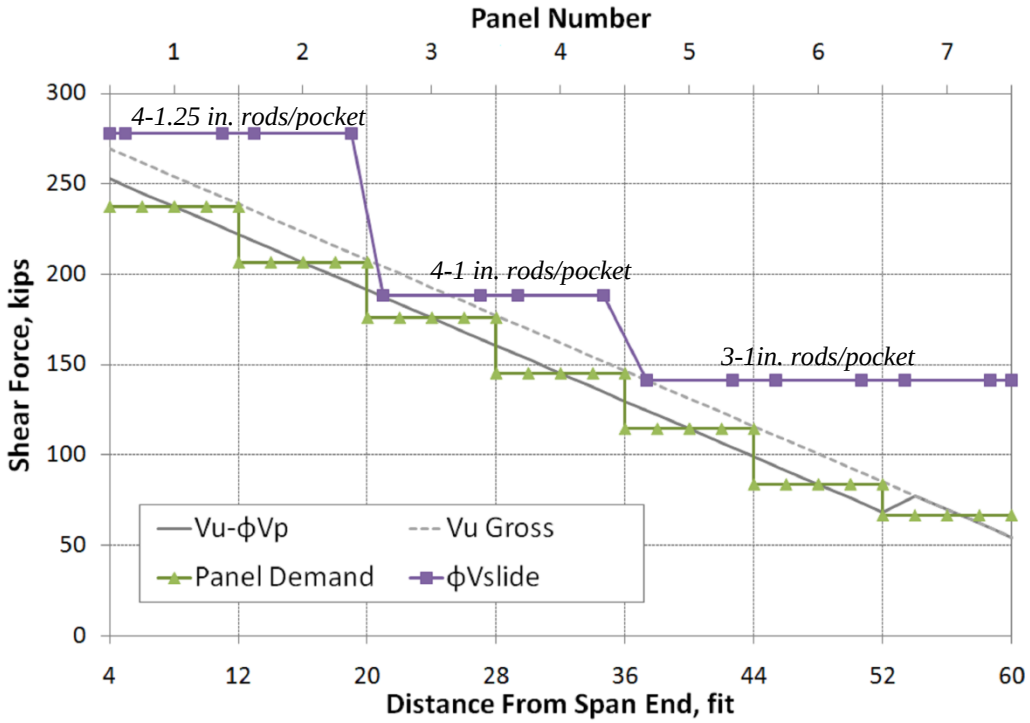

(a) Sliding shear capacity vs. demand

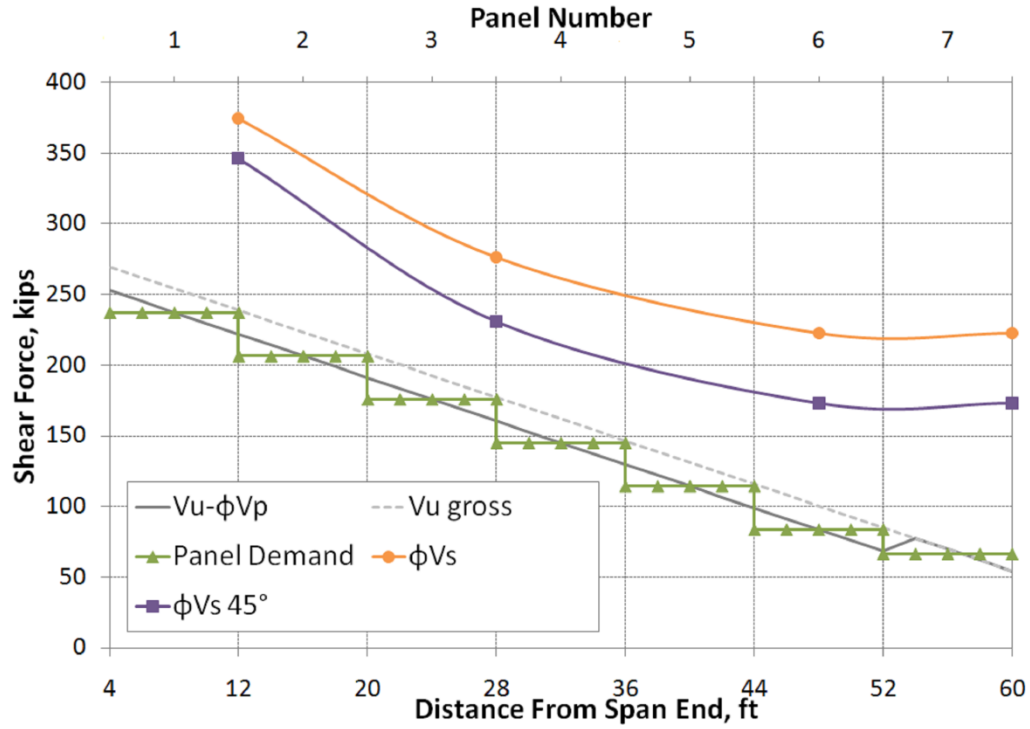

(b) Web shear capacity vs. demand

Fig. 22 – Design solution for mixed diameter shear connectors.

necessary to ensure a sliding shear failure mechanism as opposed to a brittle beam failure that can occur with little visual warning.

Experimental results from Chapter II show the ability for shear connectors to carry load out to a relative displacement of up to 1-in. Not only is this displacement large for an in-service bridge, but visual signs such a cracking in the haunch region should be visible. In the event that a bridge displaces enough to sever the connection between the deck and girder, a non-composite deck-girder system may result. On the other hand, if adequate protection is not provided against the pull-out failure mechanism, a brittle failure occurring in the girder could damage the girder enough to lead to a complete failure. Therefore, the increase in transverse reinforcement is warranted in return for the construction advantage of a full-depth deck-panel system.

If the conventional design of shear is used for the girders, as required by AASHTO (2007) in which $\phi(V_s + V_c + V_p) > V_u$ where V_c =shear carried by concrete, then it is possible that insufficient hoop reinforcement may exist along with proper placement to lead to a non-contact lap-splice. This may lead to premature beam failure as discovered by the tests conducted by Trejo et al. (2008) and Henley (2009).

3.9 Closure

The design process given in this chapter creates a constructible solution that provides adequate sliding shear capacity and ensures sufficient transverse steel is present to form a non-contact splice with the shear connectors. A design example was carried

out based on the Rock Creek Bridge, in Parker County, Texas. The key aspects of the design process are given:

1. The number of pockets in each panel are determined based on a chosen connector size and type (1-in. CR or 1.25-in. CR) to provide adequate sliding shear capacity.
2. A number of transverse hoops, N_{group}, are required to anchor the shear connectors in a pocket, forming a non-contact splice, to prevent a pull-out failure.
3. The transverse hoops associated with each pocket must also provide web shear resistance. The provided web shear resistance is always conservative due to the fact that the transverse hoops are primarily designed to anchor the shear connectors and to form the non-contact splice.
4. The inclined crack angle associated with the provided longitudinal and transverse reinforcement layout in the girder also tends to be less than 45° which engages more hoopsets and leads to additional web shear capacity.
5. The increased transverse reinforcement is a result of designing to create a sliding shear failure mechanism that is more ductile than a brittle beam shear failure.

CHAPTER IV

SUMMARY AND CONCLUSIONS

4.1 Summary

Eight single-pocket deck specimens were "pushed-off" to examine the horizontal shear-displacement performance of the deck-to-girder connection. Initial failure of the adhesive bond between the haunch and girder led to a sliding mechanism for the deck specimens. This sliding mechanism then led to yielding of the connectors and in turn provided a clamping force from which a sliding coefficient of friction was observed. The ability of this clamping force to be sustained throughout increasing displacements is dependent on the pocket grout strength. If the grout strength is sufficient a relatively constant coefficient of friction is observed to occur after the initial peak. If the grout is not of sufficient strength, the bond between the connector and pocket grout degrades leading to a decreased connector force and thus a decreased coefficient of friction.

The tests included connector specimens of threaded rod which were tested to give a common point of reference with experiments done by Henley, and coil rod connectors were tested as a possible lower cost alternative to threaded rods. Both the threaded and coil rods were tested on an I-shaped test beam to monitor effects of a narrow web.

In order for the connector system to be viable, it is key to have sufficient stirrups in the local area of the shear connectors which will allow the high pull-out force to be

resisted and prevent premature damage the girder. The amount of shear steel was increased from Henley's tests and no brittle beam failures were encountered.

The successful implementation of a full-depth precast deck-panel system requires the use of a viable design methodology that properly accounts for *system* behavior. The design of a deck-haunch-girder system used a truss modeling approach to design for the shear forces created by service loading. The truss model approach was considered more suitable for a concrete member because of the fact that the member will be substantially cracked at an ultimate limit state and that traditional beam theory does not account for the decreased ability of shear stresses to transfer across open cracks. Experimental results from Chapter II, such as the friction coefficient μ, were used along with a previously developed crack angle model to layout the geometry of the truss within a deck-panel span. Design solutions were presented using the Rock Creek Bridge in Parker County, Texas as an example structure.

4.2 Conclusions

Based on the research presented herein, the following key findings and conclusions are drawn.

1. A *systematic* experimental setup is needed to properly evaluate the performance and interaction of a deck-haunch-girder system, most notably at an ultimate limit state.

2. Although connector placement is more difficult due to reinforcing cage congestion the narrow-webbed I-girder shape showed no detrimental behavior as compared to the full rectangular beam section.
3. Closely spaced hoops in the vicinity of the connectors are necessary to ensure an effective non-contact splice. Sufficient hoop steel will allow the girder, notably the narrow-webbed girders, to carry the high pull-out forces from the connectors.
4. The lateral load capacity of the connectors is directly dependent on the net area of steel in the connection rather than the type of threads on the connector.
5. An average of μ = 0.85 in the displacement range of 0.25 to 0.5-in. was observed. However due to variability, a dependable value of μ = 0.8 is recommended for design of grout placed against hardened concrete not intentionally roughened.
6. Coil rod specimens showed similar behavior when compared to the threaded rod specimens. This demonstrates prestressed concrete based hardware that typically uses coarse threads (such as the coil rod thread bar used in this study), and is somewhat less expensive than fine thread threaded rod and high-strength bolts, may be used without any sacrifice in performance.
7. The strength of the grout in the pocket has an effect on the nature of the coefficient of friction-lateral displacement of the deck. A strong grout leads to a relatively constant coefficient of friction, and a weaker grout shows a distinct decline in the coefficient of friction as displacements are increased.

8. The number of pockets in each panel are determined based on a chosen connector size and type (i.e. 1-in. CR or 1.25-in. CR) to provide adequate sliding shear capacity.
9. A required number of transverse hoops, N_{group}, are required to anchor the shear connectors in a pocket to prevent a pull-out failure.
10. The transverse hoops associated with each pocket must also provide web shear resistance. The provided web shear resistance is always conservative

    due to the fact that the transverse hoops are primarily designed to anchor the shear connectors and to form the non-contact splice.
11. The inclined crack angle associated with the provided longitudinal and transverse reinforcement layout in the girder also tends to be less than 45° which engages more hoopsets and leads to additional web shear capacity.
12. The increased transverse reinforcement is a result of designing to create a sliding shear failure mechanism that is more ductile than a brittle beam shear failure.

4.3 Recommendations for Future Practice

Based on the experimental study and the design methodology of this thesis, recommendations for the shear connection of a full-depth precast deck-girder system are made.

From experimental data gathered in this research, the coefficient of sliding friction between a grouted haunch and a precast concrete girder, with surfaces not

intentionally roughened, should be taken as $\mu = 0.8$ when used with the undercapacity factor for shear ($\phi = 0.75$).

For design, the sliding shear resistance provided by the shear connections within a full-depth precast deck-panel shall be governed by (11), and repeated here for convenience:

$$\phi V_{slide} = \phi \mu N_p A_{sc} f_{yc} \frac{jd_o}{L_{panel}} \tag{11}$$

accompanied by the equation that governs the number of transverse hoops needed to form the non-contact splice given by:

$$N_{group} A_{sh} f_{yh} > A_{sc} f_{yc} \tag{12}$$

4.4 Recommendations for Future Research

This research provides solutions to the implementation of a full-depth precast deck-girder system, but certain aspects could be considered for future research.

1. Adding large aggregate to the grout mix used in the haunch. The use of larger aggregate in the haunch grout could lead to a higher coefficient of sliding friction and a more efficient connection.
2. Roughening of the pocket walls. The pocket walls could be roughened to create better bond between the pocket grout and deck-panel concrete to better transfer stresses created by shear connectors and possibly extending the load carry capacity of the pocket grout.

3. Effects of pocket grout on the strength and behavior of the shear connection. As discussed in subsection 2.7, distinct differences in grout strength were noted and illustrated in the behavior of the shear connection. Definitive resolution of the role that grout strength plays in the overall behavior of the shear connection is needed.

REFERENCES

AASHTO (2007). AASHTO LRFD *bridge design specification and commentary, AASHTO LRFD-07*, 4th Edition, Washington, D.C.

ACI Committee 318. (2008). *Building code requirements for structural concrete (ACI 318-08) and commentary (ACI 318-08R),* Farmington Hills, Michigan

Henley, M.D. (2009). "Shear connections for the development of a full-depth precast concrete bridge deck system." *Master of Science Thesis*, Texas A&M University, College Station, Texas.

Issa, M. A., Salas, J.S., Shabila, H.I., Alrousan, R.Z., (2006). "Composite behavior of precast concrete full-depth panels and prestressed girders." *PCI Journal*, 51(5), 132-145.

Kim, J.H., and Mander, J. (2005). "Theoretical shear strength of concrete columns due to transverse steel." *Journal of Structural Engineering, ASCE,* 131(1), 197-199.

Kim, J.H., and Mander, J. (2007). "Influence of transverse reinforcement on elastic shear stiffness of cracked concrete columns." *Engineering Structures,* 29(8), 1798-1807.

Mander, T.J., Henley, M.D., Scott, R.M., Head, M.H., Mander, J.B., and Trejo, D. (2010). "Experimental performance of full-depth precast prestressed concrete overhang bridge deck panels." *Journal of Bridge Engineering, ASCE,* http://ascelibrary.aip.org/dbt/dbt.jsp?KEY=JBENXX&Volume=1&Issue=1

Menkulasi, F., and Roberts-Wollmann C.L. (2005). "Behavior of horizontal shear connections for full-depth precast concrete bridge decks on prestressed I-girders." *PCI Journal,* 50(3), 60-73.

Scholz, D.P., Wallenfelsz, J.A., Lijeron, C., and Roberts-Wollmann, C.L. (2007). "Recommendations for the connection between full-depth precast bridge deck panel systems and precast I-beams." *Report No. 07-CR17,* Virginia Transportation Research Council, Charlottesville, Virginia.

Trejo, D., Hite, M., Mander, J., Mander, T., Henley, M., Scott, R., Ley, T., and Patil, S. (2008). *Development of a precast bridge deck overhang system for the Rock Creek Bridge*, Technical Report 0-6100-2, Texas Transportation Institute (TTI).

TXDOT (2009). "Prestressed concrete I-beam details." *Bridge Division Standards,* Texas Department of Transportation, Austin, Texas. <ftp://ftp.dot.state.tx.us/pub/txdot-info/cmd/cserve/standard/bridge/ibdstde1.pdf>

APPENDIX A

SHEAR TEST SUMMARIES

Test 1: 1-in. TR in Rectangular Beam

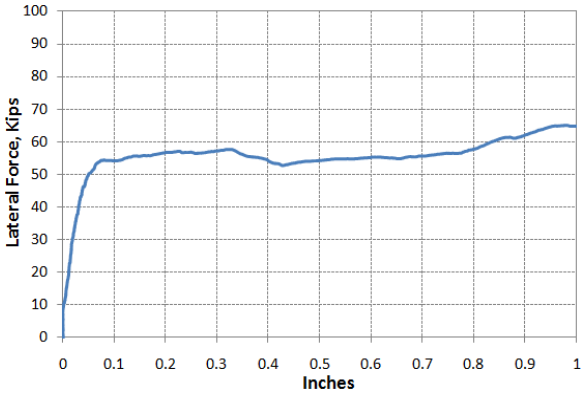

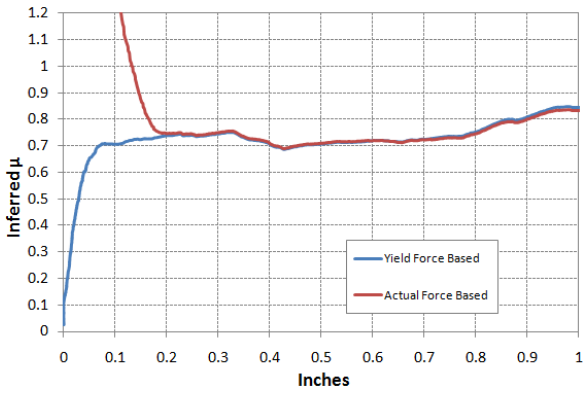

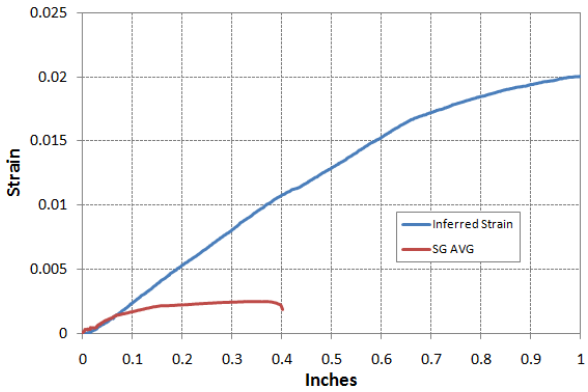

Test 2: 1-in. TR With Side-By-Side Layout in Rectangular Beam

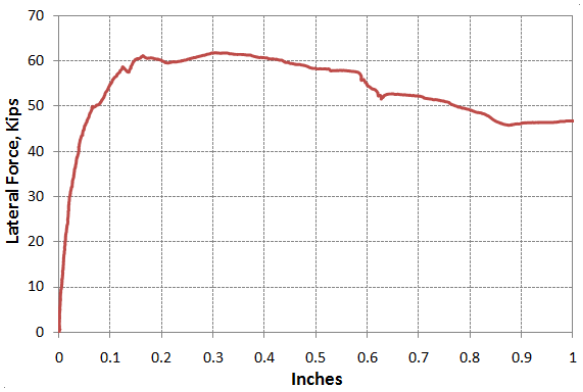

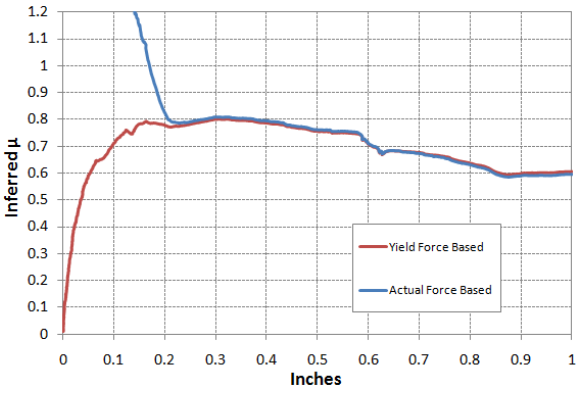

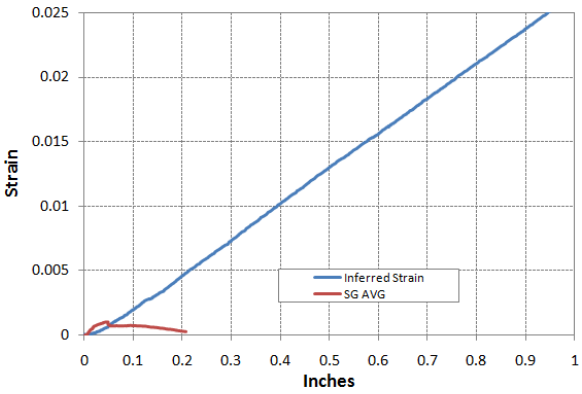

Test 3: 1-in. CR in Rectangular Beam

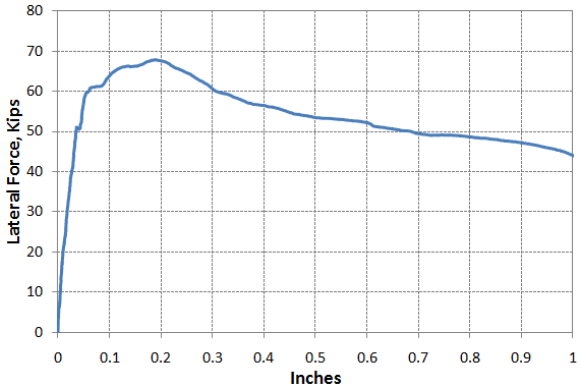

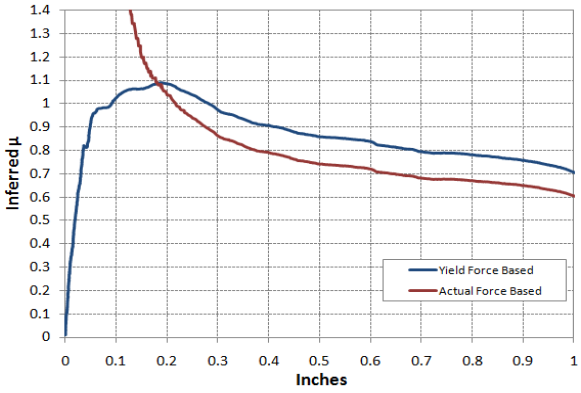

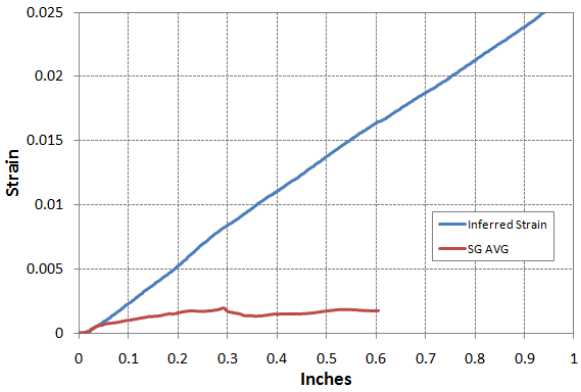

Test 4: 1.25-in. CR in Rectangular Beam

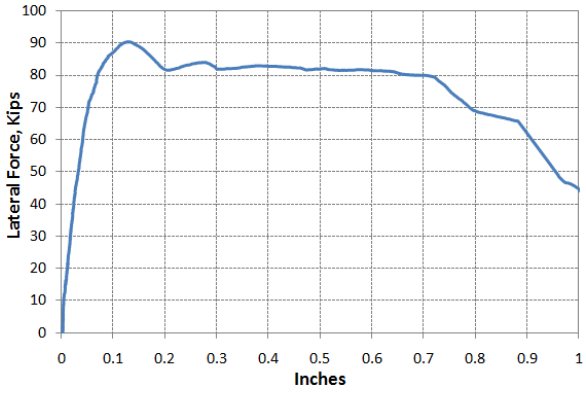

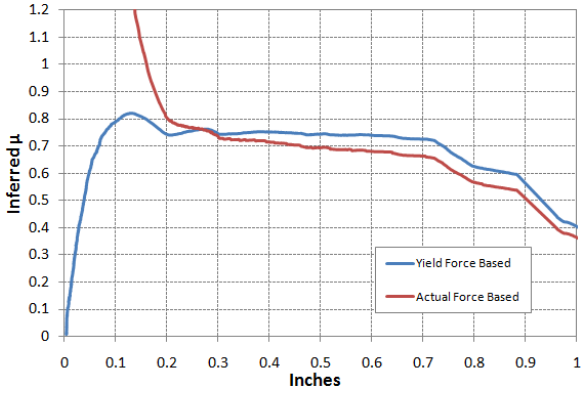

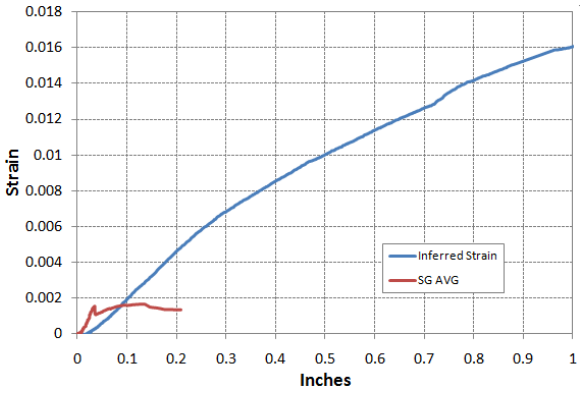

Test 5: 1-in. CR in I-Shaped Beam

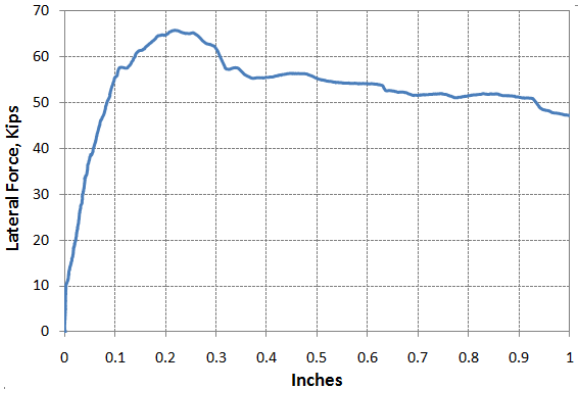

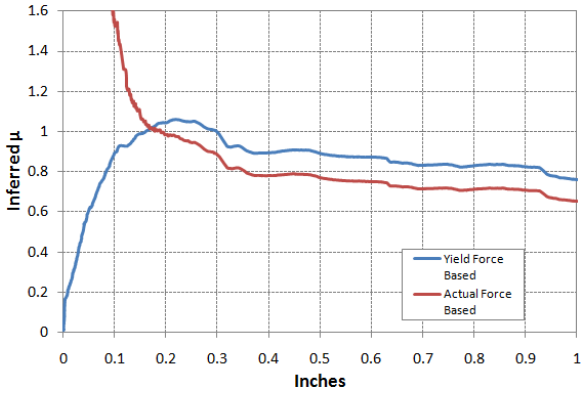

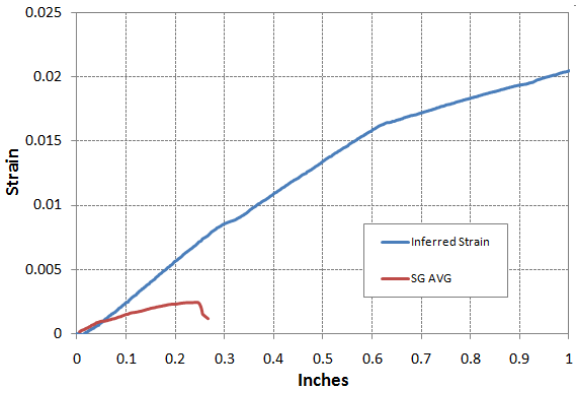

Test 6: 1-in. TR in I-Shaped Beam

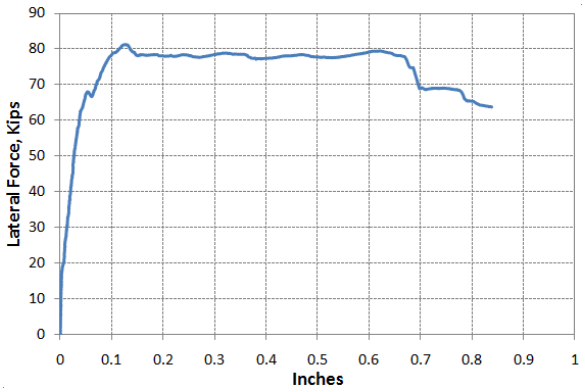

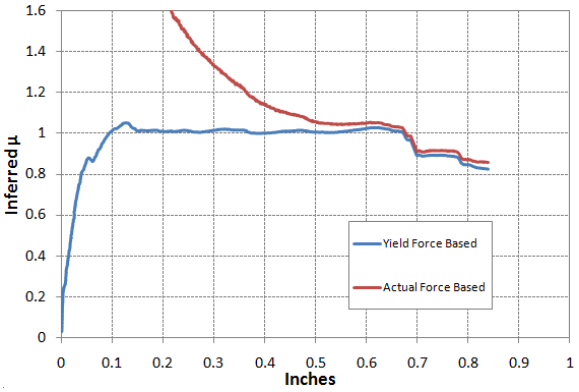

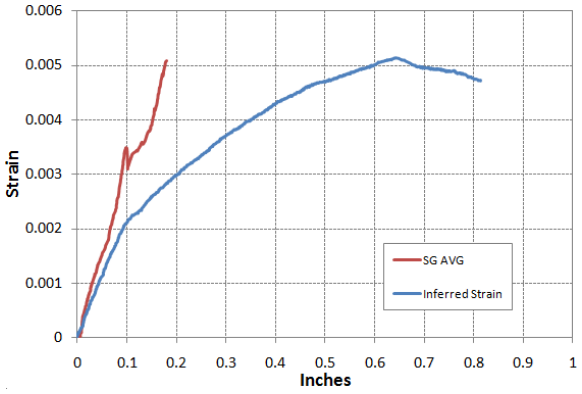

Test 7: 1-in. CR in I-Shaped Beam

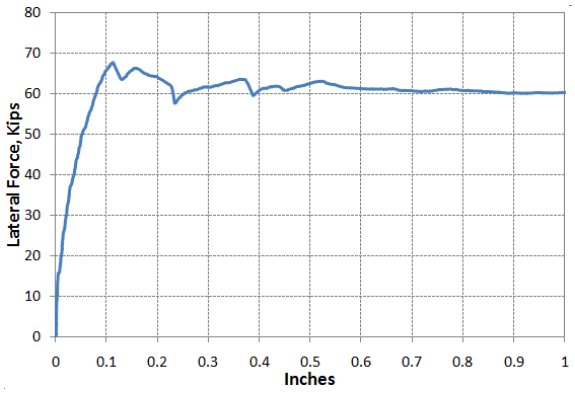

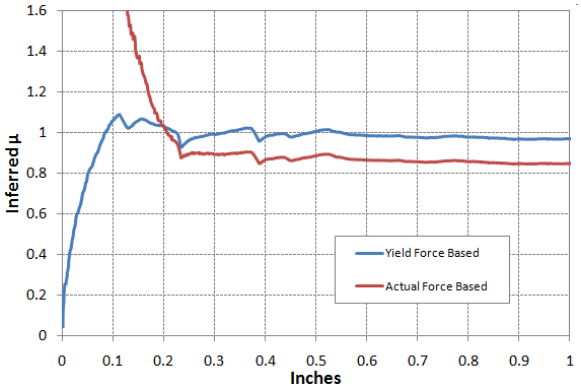

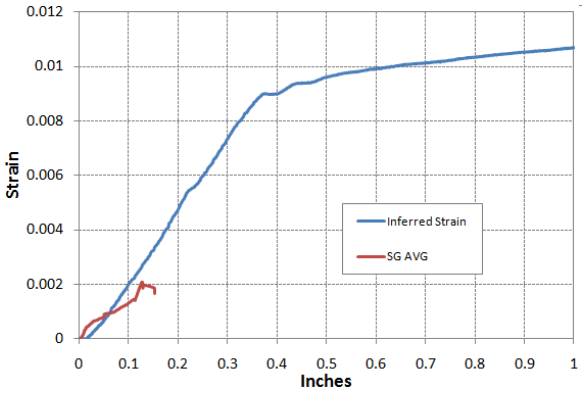

Test 8: 1.25-in. CR in I-Shaped Beam

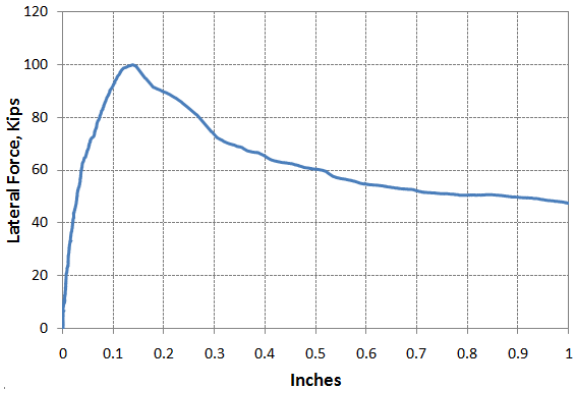

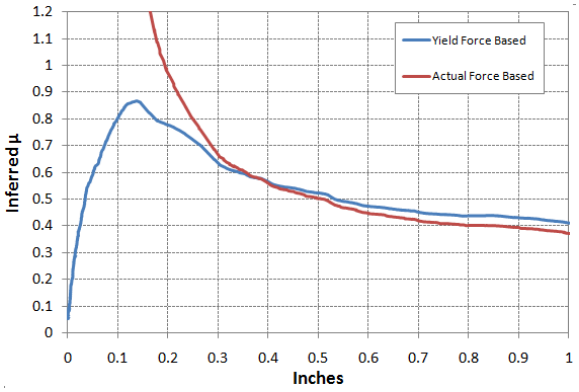

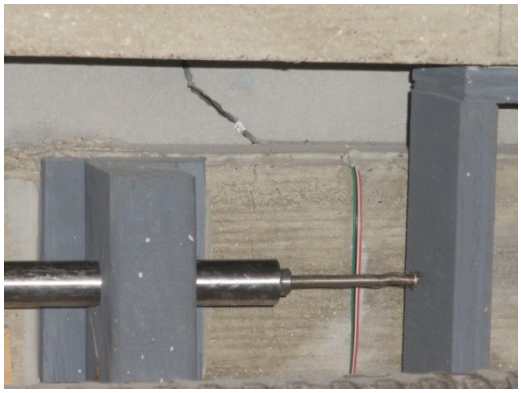

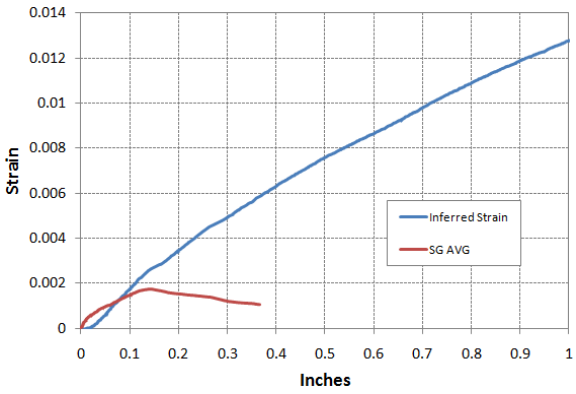

APPENDIX B

ADDITIONAL MATERIAL TESTING INFORMATION

CONCRETE STRENGTH GAIN

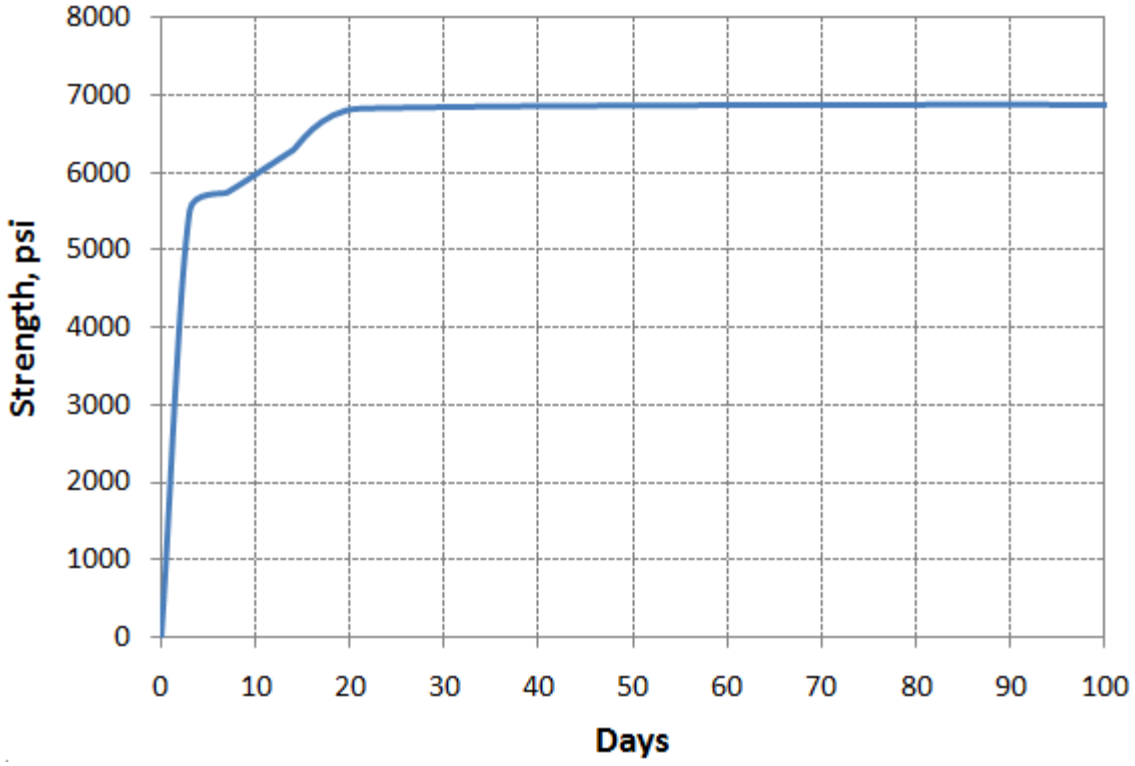

GROUT STRENGTH GAIN

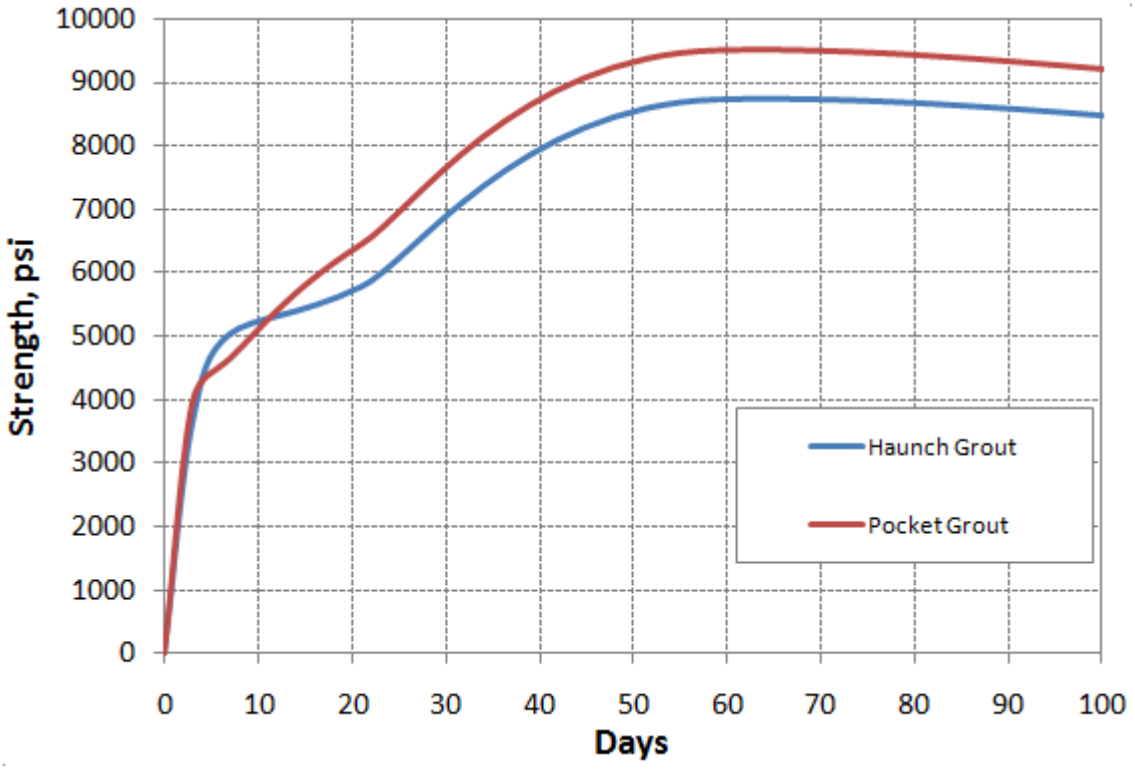

APPENDIX C

ADDITIONAL SHEAR CONNECTION DESIGN INFORMATION

Design Values Used in Chapter III

Name	Value	Comment
L	120 ft	Girder Span
ω_{DL}	1.46 kips/ft	Distributed Dead Load
ω_{LANE}	0.64 kips/ft	Distributed Lane Load
L_{panel}	96 in	Panel Length
jd_o	58 in	Overall Internal Lever Arm
jd_{girder}	49.5 in	Girder Internal Lever Arm
A_{sh}	0.62 in^2	Area of single hoop (#5)
A_{sb}	8.7 in^2	Longitudinal Girder Reinforcement
□	0.75	Shear Reduction Factor
$A_{sc,1\text{-}in.}$	1.08 in^2	Area of 2 1-in. CR
$A_{sc,\ 1.25\text{-}in.}$	1.82 in^2	Area of 2 1.25-in. CR
$f_{yc,\ 1\text{-}in.}$	120 ksi	Yield Strength of 1-in. CR
$f_{yc,\ 1.25\text{-}in.}$	105 ksi	Yield Strength of 1.25-in. CR

ROCK CREEK BRIDGE - LOADING | Z-2340 | KJ BREY

HL-93 LOADING:

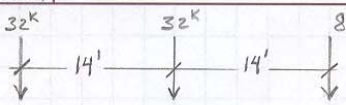

(TRUCK)

+

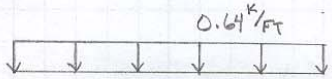

(LANE LOAD)

+

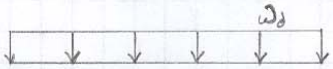

(DEAD LOADS)

DEAD LOADS:

SLAB WEIGHT — GIRDERS @ 6' C-C SPACINGS.
3' OVERANG.
6' TRIBUTARY WIDTH OF SLAB TO EXT. GIRDER.
8" SLAB

$$\omega_{SLAB} = (6\,FT)(8\,IN)\left(\frac{1\,FT}{12\,IN}\right)(0.15\,K/FT^3)$$

$$\omega_{SLAB} = 0.6\,K/FT$$

HAUNCH WEIGHT — 2IN X 20IN HAUNCH.

$$\omega_{HAUNCH} = \frac{(2\,IN)(20\,IN)(0.15\,K/FT^3)}{144\,IN^2/FT^2}$$

$$\omega_{HAUNCH} = 0.04\,K/FT$$

GIRDER WEIGHT — TYPE IV GIRDER
GROSS AREA = 788.4 IN^2 (TXDOT SPECS)

$$\omega_{GIRDER} = \frac{(788.4\,IN^2)(0.15\,K/FT^3)}{144\,IN^2/FT^2}$$

$$\omega_{GIRDER} = 0.82\,K/FT$$

$$\omega_{DL} = \omega_{SLAB} + \omega_{HAUNCH} + \omega_{GIRDER}$$

$$\omega_{DL} = 0.6\,K/FT + 0.04\,K/FT + 0.82\,K/FT$$

$$\omega_{DL} = 1.46\,K/FT$$

ROCK CREEK BRIDGE - LOADING | 2-23-10 | RJ BREY

SHEAR FROM MOVING TRUCK

FRONT WHEEL OF TRUCK @ 20', MOVING LEFT TO RIGHT.

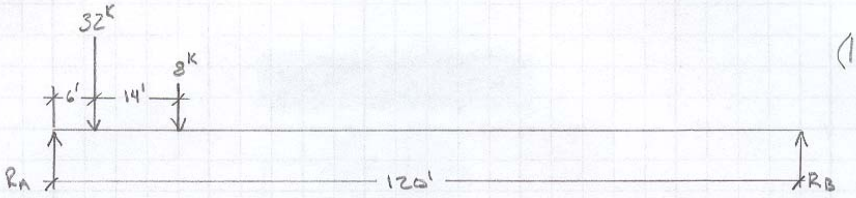

$\circlearrowleft \sum M_A$: $R_B(120\text{FT}) - (8^K)(20\text{FT}) - (32^K)(6\text{FT}) = 0$

$R_B = 2.93^K$

$\uparrow+ \sum F_Y$: $2.93^K - 32^K - 8^K + R_A = 0$

$R_A = 37.07^K$

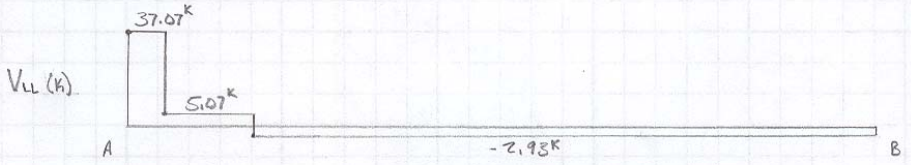

LANE LOAD SHEAR

$D_{LANE} = 0.64^K/\text{FT}$

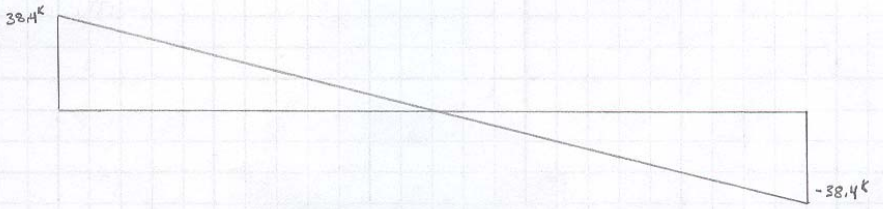

DEAD LOAD SHEAR

$D_{DL} = 1.46^K/\text{FT}$

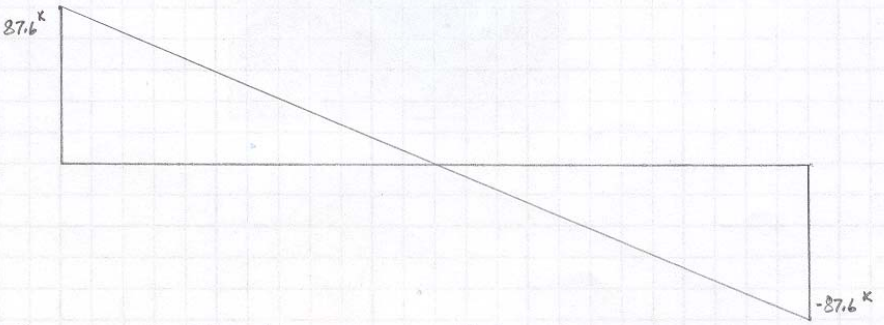

PROCESS REPEATED FOR FRONT WHEEL LOCATION @ ALL X's ALONG BRIDGE GIRDER SPAN TO PRODUCE ENVELOPE

NUMERICAL EXAMPLE – ROCK CREEK BRIDGE | 2-16-10 | RJ BREY

DISTRIBUTION OF LIVELOAD PER LANE FOR SHEAR, EXT. BEAMS.

AASHTO TABLE 4.6.2.2.3b-1 CROSS-SECTION k

(EXT) ONE LANE: LEVER RULE TWO OR MORE: $g = e g_{INT}$ $e = 0.6 + \frac{de}{10}$

(INT) ONE LANE: $0.36 + \frac{S}{25.0}$ TWO OR MORE: $0.2 + \frac{S}{12} - \left(\frac{S}{35}\right)^{2.0}$

ONE LANE, INTERIOR: $0.36 + \frac{6}{25.0} = 0.6$

TWO+ LANES, INTERIOR: $0.2 + \frac{6}{12} - \left(\frac{6}{35}\right)^{2.0} = 0.67$

ONE LANE, EXTERIOR:

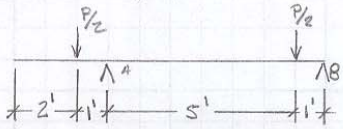

$\sum M_B: -6A + \frac{P}{2}(7) + \frac{P}{2}(1) = 0$

$\frac{4P}{6} = A \quad A = 0.67$

MULT. PRES. FACTOR: 1.2

$1.2(0.67) = 0.8$

TWO+, EXTERIOR: $e = 0.6 + \frac{2}{10} = 0.8$

$g_{EXT} = 0.8(0.67) = 0.54$

USE DF OF 0.8

LOADING/ANALYSIS

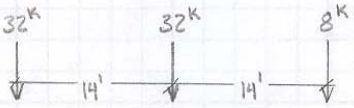

HL93

LANE LOAD: 0.64 K/FT

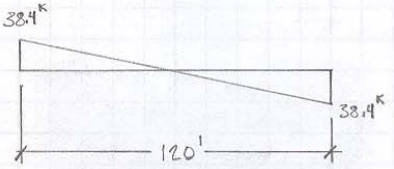

$V_U = 1.25 V_{DL} + 1.75 DF (V_{LANE} + 1.33 V_{LL})$ (STRENGTH I)

ROCK CREEK BRIDGE | 2-23-10 | RJ BREY

1.) END PANEL DESIGN FOR SLIDING SHEAR

$V_P = F_p \sin \Theta_{PS}$ Assume $f_{ps} \leq 0.75 f_{pu}$

$f_{ps} = 0.75(270\ ksi) = 202.5\ ksi$

Rock Creek Girders Contain 58 - ½" Tendons

$A_{PS} = (58)(0.15\ in^2) = 8.7\ in^2$

$F_{PS} = A_{PS} f_{ps} = (8.7\ in^2)(202.5\ ksi) = 1761.75^k$

$\Theta_{PS} = 0.73^\circ$ (From TxDOT)

$\phi V_P = (1761.75^k)\sin(0.73^\circ) = \cancel{22.4^k} \Rightarrow (0.75)(22.4^k) = \underline{16.8^k}$

$f_{pu} = 270\ ksi$

$f_{ps} = 202.5\ ksi$

$A_{TENDON} = 0.15\ in^2$

$A_{PS} = 8.7\ in^2$

$F_{PS} = 1761.75^k$

$\Theta_{PS} = 0.73^\circ$

$V_P = 22.4^k$

$\phi V_P = 16.8^k$

Harped Tendons Run $0' < X < 54'$ & $66' < X < 120'$ in Girders

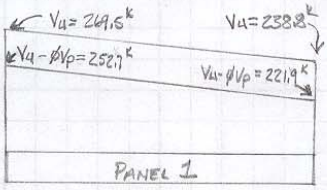

Average Shear Demand over Panel 1:

$V_{AVG} = \frac{(252.7^k) + (221.9^k)}{2}(8\ FT) = \underline{237.3^k}$ (8FT)

Panel Demand = $V_{AVG} = \underline{237.3^k}$

Panel 1 Demand = 237.3^k

Determine # of Pockets Needed in Panel 1 when using 2-1" CR/Pocket

1-1" CR has Net Cross-sectional Area of $0.541\ in^2$

$A_{SCON} = 2(0.541\ in^2) = 1.082\ in^2$

$A_{SCON} = 1.082\ in^2$

1" CR has Yield Strength of 120 ksi

$F_{YCON} = 120\ ksi$

$\phi V_{SLIDE} = \frac{\phi \mu N_{POCKET} A_{SCON} F_{YCON} jd_a}{L_{PANEL}} > \text{Panel Demand}$

$N_{POCKET} = \frac{(\text{Panel Demand}) L_{PANEL}}{\phi \mu A_{SCON} F_{YCON} jd_a} \Rightarrow \frac{(237.3^k)(96\ in)}{(0.75)(0.8)(1.082\ in^2)(120\ ksi)(58\ in)}$

$N_{POCKET} = 5.04\ \text{Pockets} \Rightarrow \underline{N_{POCKET} = 6}$

$N_{POCKET} = 6$

N_{GROUP} = # of Hoops Required to Anchor Shear Connectors in a Pocket. For 2-1" CR Shear Connectors/Pocket

$N_{GROUP} = \frac{(1.082\ in^2)(120\ ksi)}{(0.62\ in^2)(60\ ksi)}$ $N_{GROUP} = 3.49 \Rightarrow N_{GROUP} = 4$

$\phi V_{SLIDE} = 287^k$

$N_{GROUP} = 4$

2.) VERIFY THAT PROVIDED HOOPS GIVE ENOUGH RESISTANCE TO WEB SHEAR

$\phi V_S = \phi A_{SH} F_{YH} N_{GROUP} \frac{jd_{GIRDER} N_{POCKET} \cot\Theta}{L_{PANEL}}$

$\cot\Theta = 1.05\left[\frac{A_{SH} L_{PANEL}}{A_{SH} N_{GROUP} jd_{GIRDER} N_{POCKET}}\right]^{1/4}$ $\cot\Theta = 1.05\left[\frac{(8.7\ in^2)(96\ in)}{(0.62\ in^2)(4)(49.5\ in)(6)}\right]^{1/4}$

$\cot\Theta = 1.08$

ROCK CREEK BRIDGE | 2-23-10 | RJ BREY

$\phi V_S = \frac{(0.75)(0.62\,IN^2)(60\,KSI)(4)\ (49.5\,IN)(6)\ (1.08)}{(96\,IN)}$

$\phi V_S = 373^K$

$\phi V_S > V_U$ ✓

$\phi V_S = 373^K$

NOTE: 1-1¼" CR HAS A NET CROSS-SECTIONAL AREA OF $0.91\,IN^2$
2-1¼" CR HAS $1.82\,IN^2$

YIELD STRENGTH OF 1¼" CR IS 105 KSI

N_{GROUP} REQUIRED FOR 2-1¼" CR/POCKET:

$N_{GROUP} = \frac{(1.82\,IN^2)(105\,KSI)}{(0.62\,IN^2)(60\,KSI)} = 5.14 \Rightarrow N_{GROUP} = 6$

2-LEGGED #5 HOOPS ARE USED IN ALL CALCULATIONS.
$A_{SH} = 0.62\,IN^2$ $F_{YSH} = 60\,KSI$

$A_{SH} = 0.62\,IN^2$
$F_{YSH} = 60\,KSI$

VITA

Robert Wayne Brey Jr. received his Bachelor of Science degree in civil engineering from Texas A&M University in August 2008. He entered the structures program at Texas A&M University in August 2008 and received his Master of Science degree in May 2010. He will work as a project engineer at a structural engineering firm in Lindale, Texas beginning March 2010.

Robert Brey can be reached at PO Box 1348, Lindale, TX, 75771. His email address is breyrw@neo.tamu.edu.